ABSTRACT

BIOMECHANICAL TESTING OF UPRIGHT RANGE OF MOTION VERSUS OVERHEAD SUPINE RANGE OF MOTION

by
Linda Uko

Rehabilitation of an elbow, following injury, is not a well-studied subject. Clinically, there is not a general consensus on which recovery method is optimal for healing an unstable elbow. When dealing with medial collateral ligament deficiency, many authors have proposed several forearm positions that will yield proper healing of the unstable elbow. Some researchers believe that active mobilization of the elbow with the arm in a vertical position is a safe protocol for rehabilitation with the forearm oriented in a supine pronated position. It was also mentioned that the compressive forces due to the active mobilization of the arm will stabilize the MCL deficient elbow[1]. This study is unique in that the proposal is that supine overhead range of motion will stabilize the MCL deficient elbow because gravity will act as a compressive force keeping the MCL deficient elbow intact. In this study, the gravitational stabilizing factor will be demonstrated comparing both the supine overhead range of motion and the commonly used upright range of motion protocol. The hypothesis is that supine overhead range of motion provides stability to a collateral deficient elbow. Moreover, supine overhead range of motion is a superior way to rehabilitate an unstable elbow because the forces of gravity hold the elbow in concentric reduction rather than distracting the elbow joint when the forearm is rehabilitated in an upright manner. The overhead ROM provided more stability to the unstable elbow, more especially to the elbows with the AC still intact.

BIOMECHANICAL TESTING OF UPRIGHT RANGE OF MOTION VERSUS OVERHEAD SUPINE RANGE OF MOTION

by
Linda Uko

A Thesis
Submitted to the Faculty of
New Jersey Institute of Technology
in Partial Fulfillment of the Requirements for the Degree of
Master of Science in Biomedical Engineering

Department of Biomedical Engineering

August 2008

Blank Page

APPROVAL PAGE

BIOMECHANICAL TESTING OF UPRIGHT RANGE OF MOTION VERSUS OVERHEAD SUPINE RANGE OF MOTION

Linda Uko

8/21/08

Dr. Virak Tan, M.D. Thesis Co-Advisor — Date
Associate Professor of Orthopaedics, UMDNJ

8/21/08

Dr. Richard Foulds, PhD, Thesis Co-Advisor — Date
Professor of Biomedical Engineering, NJIT

8/21/08

Dr. Sergei Adamovich, PhD, Committee Member — Date
Assistant Professor of Biomedical Engineering, NJIT

BIOGRAPHICAL SKETCH

Author: Linda Arit Uko

Degree: Master of Science

Date: August 2008

Undergraduate and Graduate Education:

- Master of Science in Biomedical Engineering,
  New Jersey Institute of Technology, Newark, New Jersey, USA, 2008

- Bachelor of Science in Biomedical Engineering,
  Boston University, Boston, Massachusetts, USA, 2005

Major: Biomedical Engineering

Presentation:

Linda A. Uko and Alexander Adam,
"Characterize an EMG Signal from a Prototype Surface Array Electrode,"
The Sixth Annual Biomedical Engineering Symposium
Biomedical Engineering (BME '05), Boston, MA, May 2005.

To my beloved family

Thanks for all of your prayers, support and concern regarding my thesis. You gave me the strength to start it, to continue it and to complete it. You all were supportive and motivate me when I was struggling. You all even offered to help, knowing that there was not much you could do. I thank you from the bottom of my heart.

ACKNOWLEDGMENT

I would like to extend my deepest gratitude to my advisor Dr. Virak Tan for his support throughout the duration of my research. He was supportive in his efforts, patient, willing to help and resourceful. I also express my appreciation to, soon to be, Surgeon Sydney Pardino, who was an integral part to the completion of my project. Regardless of how many hours he slept, he never waned in spirit, he was always willing to assist me and he always made sure that I was equipped with the necessary resources I needed to execute my tests. I give my special thanks to Dr. Foulds who helped me with the technical portion of my thesis. I thank the University of Medicine and Dentistry of New Jersey for funding this project. I give my deepest thanks to Kai Chen. He provided great technical and educational support on programming of this project. I express my gratitude to Linda Chen, who stepped in during the latter part of my thesis and help with data extraction, testing and preparation. She was a great support system.

I give thanks to my Lord and Savior Jesus Christ for making me to fulfill this project. I give thanks to my family, especially my mother who gave me words of encouragement and hope. My thanks goes to Biosio Etim who stayed up with me those late nights while I was working on my thesis, for the trips back and forth to the hospital, transporting my equipment. He motivated me even when I was weak and he always pushed me to do well. Last but not least, I extend my thanks to Omosola Osunfisan and Jennifer Ezirike for their prayers and support.

TABLE OF CONTENTS

TABLE OF CONTENTS
(Continued)

Chapter **Page**

TABLE OF CONTENTS
(Continued)

Chapter **Page**

LIST OF TABLES

Table **Page**

LIST OF FIGURES

LIST OF FIGURES
(Continued)

Figure **Page**

LIST OF FIGURES
(Continued)

Figure **Page**

LIST OF SYMBOLS

Symbol	Definition
c	cosine
s	sine
AC	anterior capsule
CP	Coronoid Process
EL	Lateral epicondyle
EM	Medial epicondyle
LCL	lateral collateral ligament
LT	Listers Tubercle
MCL	medial collateral ligament
OL	Olecranon
OT	Midshaft
RH	Radial Head
ROM	range of motion
RS	Radial Styloid
US	Ulnar Styloid

CHAPTER 1

INTRODUCTION

1.1 Objective

The objective of this thesis is to determine which rehabilitation protocol for subjects with medial collateral ligament deficiency and/or lateral collateral ligament deficiency provides the patient with optimal healing of the elbow. This will be demonstrated using biomechanical testing of cadaver bones with medial collateral and lateral ligament deficiencies in both an upright supine range of motion compared to overhead range of motion.

1.2 Background Information

1.2.1 Anatomy of the Elbow

The elbow joint is comprised of the ulna, humerus and the radius.

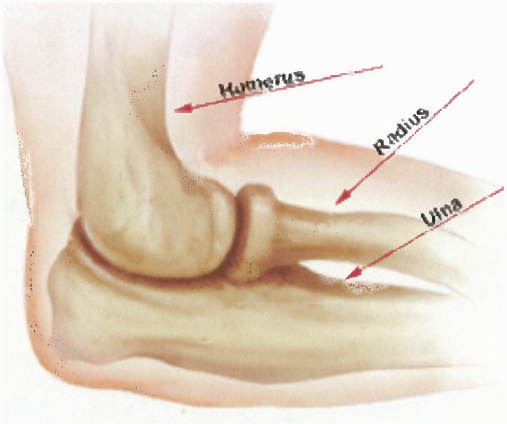

Figure 1.1 The side view of the elbow joint, containing the humerus, radius and ulna bones[12]

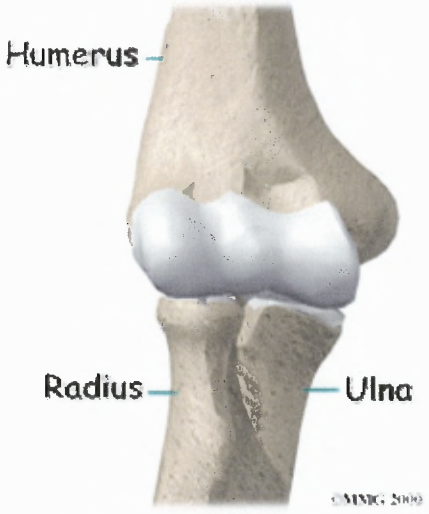

Figure 1.2 The frontal view of the three bones that comprises the elbow joint [12]

The elbow is a complex joint that allows for two types of motion: flexion-extension and pronation and supination. The structures of the elbow that are responsible for the flexion and extension of the forearm are the ulnohumeral and radiocapitellar (ie radiohumeral) articulations. The proximal radioulnar articulation controls the pronation and supination movement. The elbow is referred to as a trochleoginglymoid joint because of its hinged nature and because of its ability to flex and extend.

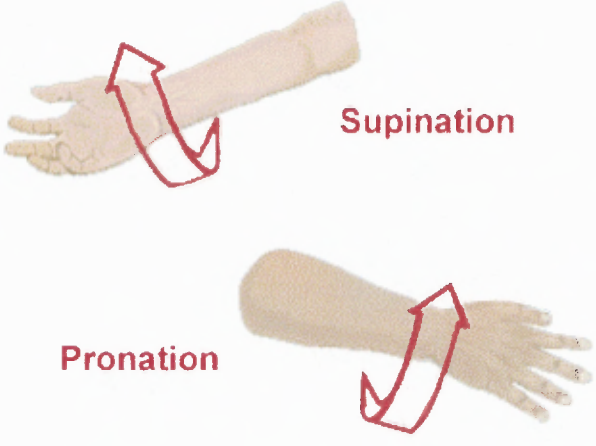

Figure 1.3 An illustration of the types of rotations that are performed by the forearm: Supination (Palm facing upwards), Pronation (Palm facing downwards)[16]

The standard range for flexion and extension is from 0 degrees to 145 degrees. The normal arc of pronation and supination is approximately 180 degrees – 90 degrees in each direction. The elbow can operate within a functional range of 50 degrees each in supination and pronation, and with an extension-flexion arc from a flexion contracture of 30 degrees to flexion of 130 degrees.

1.2.2 Elbow Stability

The elbow is stabilized by several factors; ligaments, gravitational stabilizers, muscles of the elbow, contact forces and the morphology of the elbow. The medial collateral ligament is a complex that comprises of an anterior bundle, a posterior bundle and a transverse ligament. The anterior bundle and the posterior bundle work in conjunction to provide stability to the elbow. The anterior bundle tightens in extension meanwhile the posterior bundle tightens during flexion[17]. The anterior bundle of the MCL serves as the primary valgus stabilizer of the elbow meanwhile the radial head serves as the secondary constraint[14]. In this study, the stability maintained between the humerus and ulna will be the main focus because the morphology of the ulna provides for better stability and the motion of the radius presents a more complicated motion. Calculation from the motion of the radius will serve as a check for the flexion and extension angles.

1.2.3 Medial Collateral Deficient Elbow

MCL deficiency is usually a result of thrower's elbow, in which the acceleration stage of pitching produces high tensile stress to the ligament producing attenuation or a slight rupture of the MCL[4].

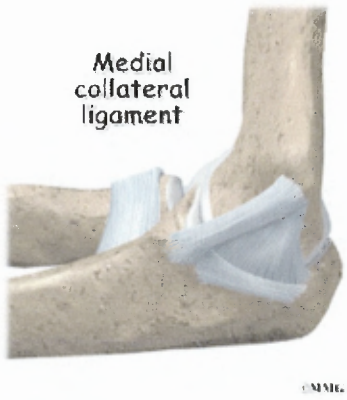

Figure 1.4 The medial collateral ligament is the primary stabilizer of the elbow joint [19]

1.2.4 Lateral Collateral Ligament

The lateral collateral ligament is comprised of the radial collateral ligament that stems from the lateral epicondyle. The lateral collateral ligament has its origin at the center of the axis of elbow rotation and thereby responsible for maintaining the length of the ulna throughout the flexion/extension arc of motion. The lateral collateral ligament has also been reported as a stabilizer of the ulnohumeral joint with active varus and external rotation.

Figure 1.5 The lateral collateral ligament that serves as one of the stabilizers of the elbow joint [18]

1.2.5 Overhead Elbow Exercises

The rehabilitation goal for any unstable elbow is to restore motion, yet allow the damaged ligaments to heal properly. Thus, early elbow motion is necessary to prevent stiffness. The overhead elbow exercises are done laying flat on your back. The subject places their arm over their chest and the splint is removed while the elbow remains bent. The bent elbow is then positioned directly over the shoulder, keeping the steady arm perpendicular to the floor. The subject proceeds to straighten the elbow and can use the free hand to support and straighten the injured arm. The subject then bends their elbow back down towards the chest. This procedure is repeated for ten repetitions. The subject has to rotate the forearm by bending the elbow at a 90 degree angle so that the palm is facing away from the subject. This position must be kept for 10 seconds. The subject then rotates the forearm in the opposite direction so that their palm is facing downwards. This position is also held for ten seconds. The free hand may be used as support for this process. This must be repeated for ten repetitions. At the completion of the exercises, the elbow splint is put back onto the elbow[18].

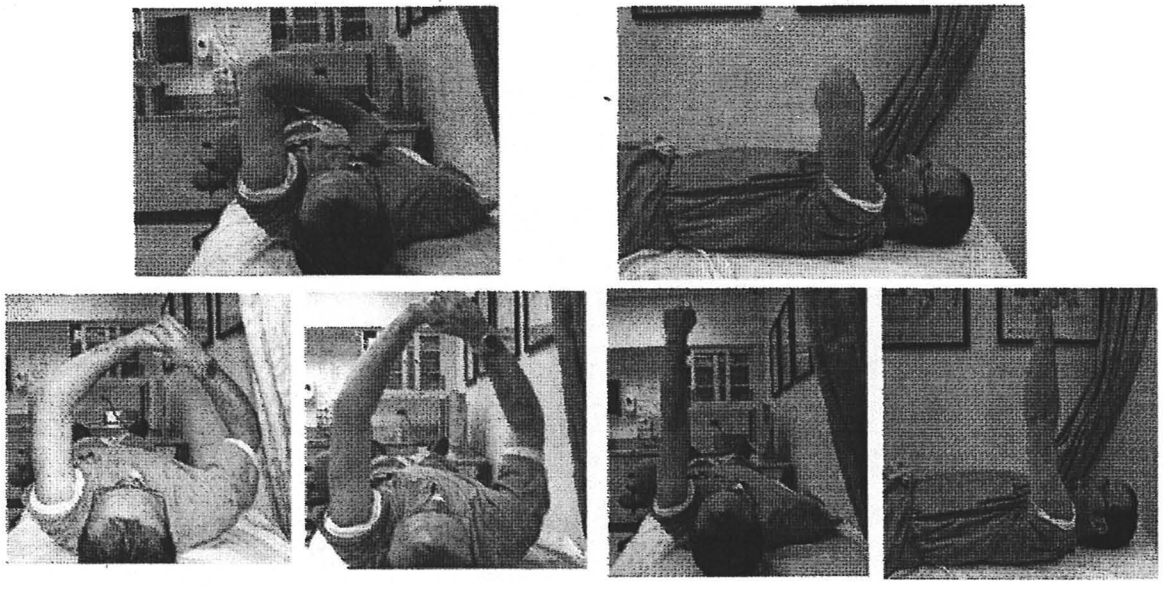

Figure 1.6 Overhead Elbow Exercises

1.2.6 Flock of Birds Ascension Technology

The elbow instability will be measured using the following outcome variables: 1) displacement of the proximal ulna relative to the distal humerus, 2) ulnohumeral angles (roll, pitch, yaw angles) at which elbow instability takes place during range of motion (ROM). These parameters will be measured using the Flock of Birds (FOB) electromagnetic tracking device[19]. FOB provides six degrees of freedom information of both position and orientation of a sensor relative to its transmitter. The transmitter is capable of tracking the position and orientation of up to 30 sensors simultaneously. FOB is able to provide these outputs by transmitting a pulsed DC magnetic field that is measured by the applied sensors. Based on the magnetic field characteristics, the sensor is able to provide positional and orientational outputs and make it available to the host computer [19].

Figure 1.7 The Flock of Birds Ascension Technology: contains the transmitter, as well as the sensors used in tracking position and orientation. [19]

The Flock of Birds Ascension Technology unit was coupled with a software program, WINBIRD. Figure 1.7 shows the setup of the program used to calculate the orientation of the sensor.

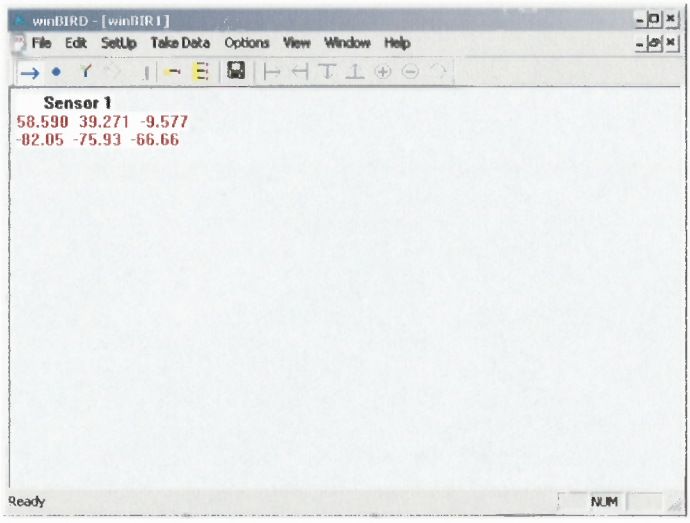

Figure 1.8 WINBIRD is a program coupled with Flock of Birds for data collection from the sensors.

The program can be used with up to two sensors in order to extract the rotational (roll, pitch and yaw) and positional (x,y,z) values obtained by the Flock of Birds unit. The user is also allowed to set up the system to allow for the data extraction of one or multiple sensors.

CHAPTER 2

METHODS AND MATERIALS

2.1 Testing Apparatus

A wooden jig was constructed with two board pieces attached by way of four wooden pegs. This provided rotational freedom to test the specimen in both upright and overhead range of motion without repositioning the transmitter. This maintained the coordinate systems of the bones fixed relative to the transmitter's coordinate system. . It contained two custom clamps on the wooden jig that rigidly held the humerus in place. Two holes were drilled into the humerus and stainless steel pins were used to hold the humerus between the clamps. The transmitter was securely placed proximal to the humerus. Another hole was drilled into the proximal humerus. Two sensors were used in this experiment; one sensor was fixed, with two plastic screws, to the distal end of the radius, meanwhile the second sensor was fixed to the distal portion of the ulna. The second sensor was similarly screwed onto the ulna. Since the humerus was fixed and stationed at neutral position, the sensor was used to take the rotational and positional values of the humerus before the sensors were attached to the radius and ulna.

2.2 Cadaveric Specimens

The six cadaver arms were stored at -20 degrees Celsius and precut at the mid humerus. The elbow was still intact and the bones were exposed. The specimens were given 12 hours to thaw prior to testing. Holes were drilled into the specimens in order to mount the specimen to the testing apparatus. Three holes were drilled into the humerus and securely mounted in order to prevent movement of the humerus. Two holes were drilled onto the distal end of the

ulna where the Flock of Birds sensor was attached. Both right and left elbows were used in this experiment.

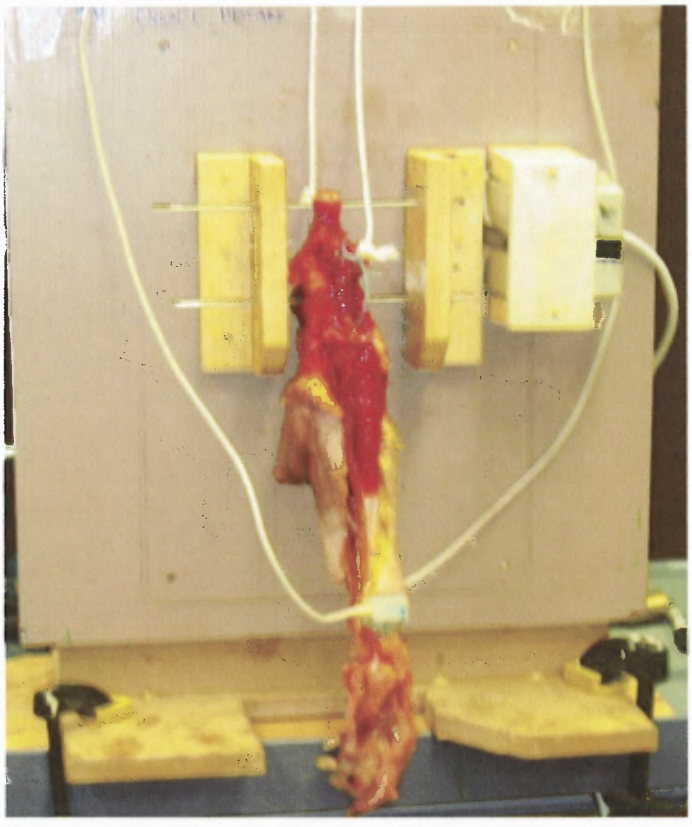

Figure 2.1 Actual View of a Specimen with FOB sensors attached with a transmitter fixed into position

2.3 Testing of a Specimen with Both Radius and Ulna Intact

One Flock of Bird receiver was mounted onto the ulna and the other receiver was mounted onto the radius. The arm was oriented in an upright position with the forearm completely extended (according to the maximum extension capability of each specimen). During the passive range of motion, the arm was passively moved from full extension to complete flexion and back to complete extension; completing one cycle. The jig was then rotated, placing the arm in overhead ROM. The arm was passively moved from full overhead extension to maximum flexion and back to maximum extension. The jig was rotated,

positioning the arm in supine upright ROM. To simulate active motion, #5 caliber nonabsorbable sutures were attached to the brachialis and triceps tendons and passed through pulleys. 2- two kilogram weights were attached to each suture to replicate muscle tone. Active elbow flexion is achieved by applying a force to the brachialis suture and active extension by a force on triceps. The jig was rotated and active motion was performed with the forearm in overhead ROM and the motion going from full extension to full flexion. This process was executed when 1) Ligaments were intact 2) MCL ligament was severed 3) MCL, LCL ligaments severed 3) MCL, LCL, AC ligaments severed. In this order were the ligaments severed. At the completion of the trials, the elbow was disarticulated and the landmarks of the arm were collected using a stylus.

2.4 Calibration of the Stylus

A centering program was created using Natick Mathworks MATLAB program in order to calibrate the stylus and obtain the offset lengths of the tip from the center of the sensor. The zero point of the stylus on the sensor was obtained and the stylus was rotated at 45 degrees.

2.5 The Procedure for Computing Angles from the Flock of Birds Sensors

The Flock of Birds Sensor provides information about the orientation and position of the sensor relative to the transmitter. In order to compute the angle of the ulna and radius relative to the receiver, a series of transformations need to be performed. Figure 2.2 shows the series of steps needed to compute the angles of the ulna and radius relative to the humerus.

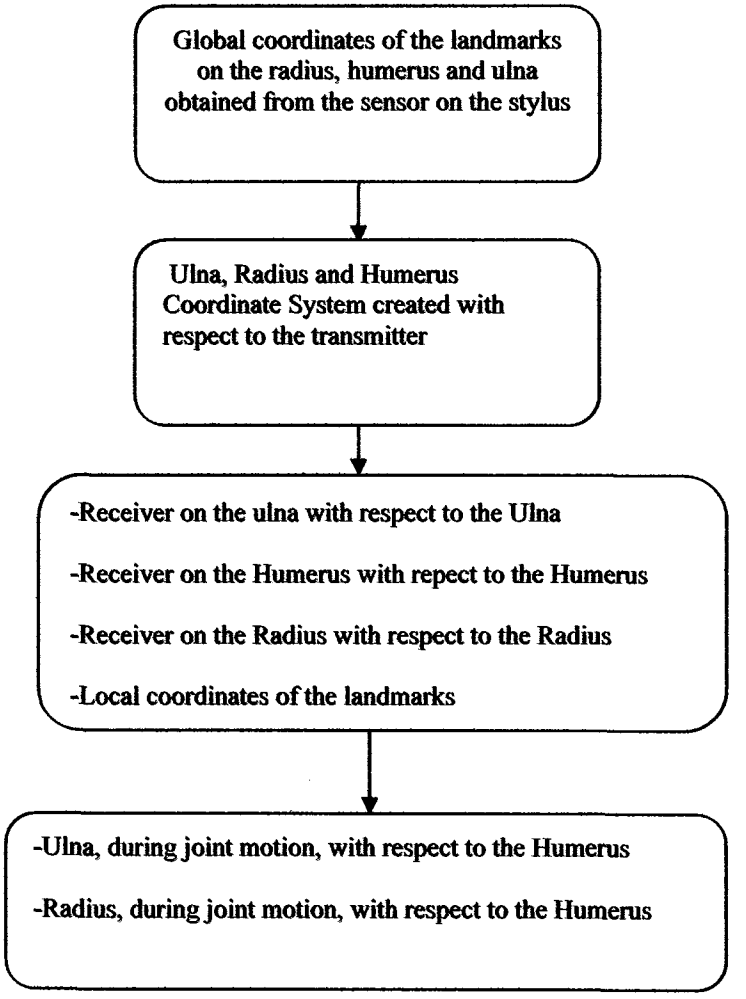

Figure 2.2 Extraction of Kinematic Data during Joint Motion

2.6 Kinematic Data

The Flock of Birds kinematic data of the two sensors were obtained. The two sensors provided the x, y, z displacement values of the sensors relative to the transmitter. It also yielded the rotational values; roll, pitch and yaw of the sensors relative to the transmitter.

An anatomical Cartesian coordinate system of each bone was constructed to allow the data obtained from the Flock of Birds to quantify the motion pathways of the ulna relative to the humerus. The skin was removed from the arm and each of the bones was disarticulated. The bony landmarks of each bone were identified using palpitation methods. The bony landmarks that were chosen for the humerus were the midshaft, the medial epicondyle and the lateral epicondyle. The landmarks that were chosen for the radial bone were the radial styloid, lister's tubercle, and the radial head. The bony landmarks of the ulna were the ulnar styloid, coronoid process, and the olecranon. The kinematic data for the landmarks were obtained using a 93.668 millimeter stainless steel styloid securely attached to the sensor.

Using coordinate system transformation, the motion pathways were quantified for the ulna relative to the humerus. First the landmarks of the humerus were used to create a Cartesian coordinate system in which the x axis was formed with the medial epicondyle (EM) and the lateral epicondyle (EL). The z-axis, which is considered in the plane of the ulnar motion, was formed using the cross product of the distance from the midshaft and the midpoint between the lateral and medial epicondyle. The y-axis was formed by the cross product of the z-axis and the midpoint between the olecranon and the coronoid process. The x-axis of the ulna was formed by the cross product of z-axis and the y-axis.

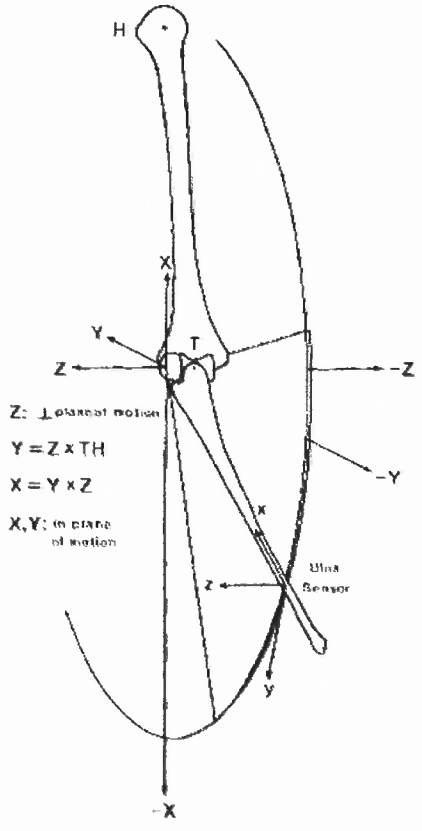

Figure 2.3 The coordinate system used to define the ulna and the humerus. HT refers to the long axis of the humerus (from the humerus to the midpoint of the EM and EL). Z is the flexion axis and when crossed with HT provides the Y axis. The X axis is generated from the cross product of the Y and Z axis[14].

Once the anatomical coordinate systems were formed, a transformation matrix of the ulna relative to the sensor was formed as well as the transformation matrix of the humerus with respect to the transmitter. Through coordinate system transformations, the motion of the ulna is described relative to the humerus. The coordinate system transformations will provide information about the rotational changes occurring in the ulna relative to the humerus as well as the changes in displacement at the elbow joint.

2.7 Kinematic Calculation

Table 2.1 is the derivation of the coordinate system for the humerus, ulna and radius were created from the landmarks collected.

Table 2.1 Mathematical Derivation of Bone Coordinate Systems

Bone	**Landmarks**	**Coordinate System**
Humerus	Midshaft **(MS)**	Z axis: MS-((EM+EL)/2) || MS-((EM+EL)/2)||
	Medial Epicondyle **(EM)**	Y axis: Z **X** (CP+OL)/2 || Z **X** (CP+OL)/2||
	Lateral Epicondyle **(EL)**	X axis: Z **X** Y || Z **X** Y||
Ulna	Ulnar Styloid **(US)**	Z axis: CP-US || CP-US||
	Olecranon **(OL)**	Y axis: Z **X** (CP-OL) ||Z **X** (CP-OL)||
	Coronoid Process **(CP)**	X axis: Z **X** Y || Z **X** Y||
Radius	Radial Styloid **(RS)**	Z axis: RH-RS || RH-RS||
	Listers Tubercle **(LT)**	Y axis: Z **X** (RS-LT) || Z **X** (RS-LT)||
	Radial Head **(RH)**	X axis: Z **X** Y || Z **X** Y||

2.7.1 Euler's Angle Computation

Euler's angles are used to describe the orientation of one coordinate system relative to another coordinate system. The Euler's angles are used to describe the orientation of the moving ulna coordinate system relative to the humerus coordinate system and the radial coordinate system relative to the ulna coordinate system. The Euler's angles are sequence dependent and are a sequence of ordered rotations from the initial position of the ulna coordinate system[20]. The rotation matrix for the ZYX order is:

$$[R]=[Rz][Ry][Rx] \tag{2.1}$$

$$Rz=\begin{vmatrix}1 & 0 & 0\\ 0 & c\gamma & -s\gamma\\ 0 & s\gamma & c\gamma\end{vmatrix} \quad Ry=\begin{vmatrix}c\beta & 0 & s\beta\\ 0 & 1 & 0\\ -s\beta & 0 & c\beta\end{vmatrix} \quad Rz=\begin{vmatrix}c\alpha & -s\alpha & 0\\ s\alpha & c\alpha & 0\\ 0 & 0 & 1\end{vmatrix} \tag{2.2}$$

$$[R]=\begin{vmatrix}c\beta c\gamma & c\gamma s\beta s\alpha + s\gamma c\alpha & s\gamma s\alpha - c\gamma s\beta c\alpha\\ -s\gamma c\beta & c\alpha c\gamma - s\alpha s\beta s\gamma & s\gamma s\beta c\alpha + c\gamma s\alpha\\ s\beta & -c\beta s\alpha & c\alpha c\beta\end{vmatrix} \tag{2.3}$$

Abduction/Adduction about the y axis: $\beta=\sin\text{-}1(R_{31})$ (2.4)

Flexion/Extension about the x axis: $\alpha=\dfrac{\sin^{-1}(R_{23})}{\cos\beta}$ (2.5)

Internal/External Rotation about the z axis: $\gamma=\dfrac{\sin^{-1}(R_{12})}{\cos\beta}$ (2.6)

MATLAB software was used to calculate the subsequent rotations and the details of this computation are found in Appendix B.

2.7.2 Coordinate System of Flock of Birds System

The Flock of bird transmitter and the Flock of Bird sensors has the same coordinate system. The transmitter represents the global coordinate system in which the sensor's local coordinate system is based upon. The position and rotation of each sensor is relative to the transmitter's coordinate system. The Flock of Bird's system uses Euler angles to define the rotation of each sensor relative to the transmitter.

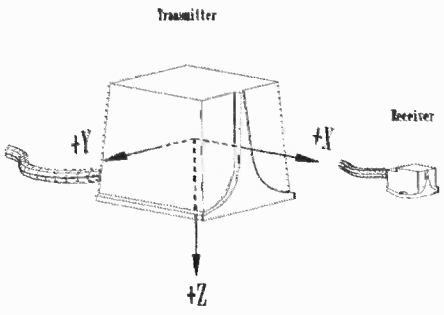

Figure 2.4 The coordinate system of the Flock of Birds Transmitter and its receiver[20].

2.7.3 Gimbal Lock

Gimbal lock is a problem that occurs when Euler angles are implemented. It is a phenomenon whereby two axis of rotation are equivalent to one another or pointing in the same direction. In this study, gimbal lock was avoided by careful attention to the nature of the forearm's movement in order to avoid discrepancies in the data.

2.7.4 Data Processing

Figure 2.5 shows the process by which information from the Flock of Bird is transmitted in order to extract the rotation and positional values during joint motion.

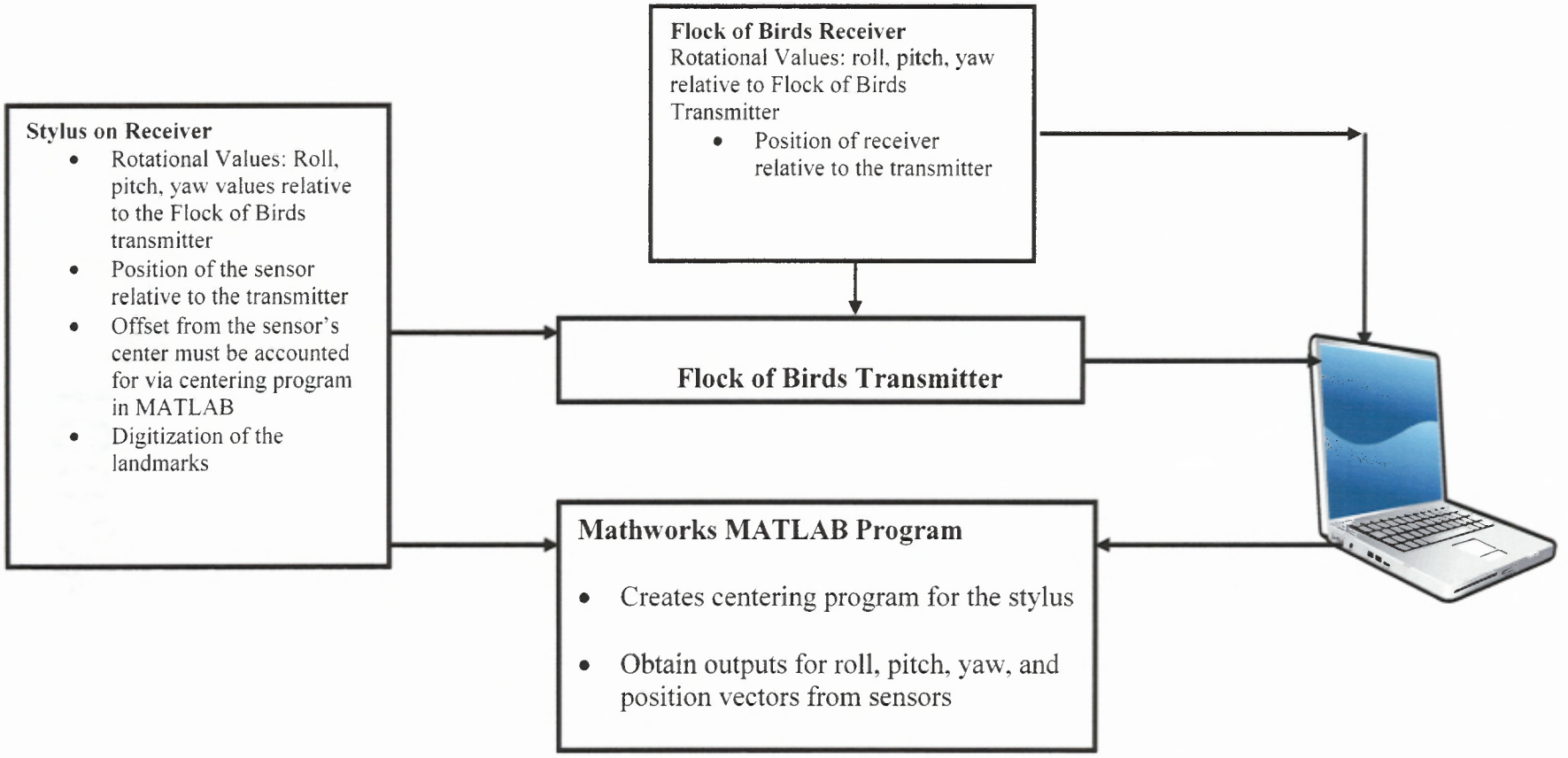

Figure 2.5 Data Processing of the Flock of Birds Ascension Technology Sensor

CHAPTER 3

RESULTS

3.1 Sectioning of the Ligaments during the Experimental Protocol

The experiment was performed where the sectioning of the ligaments was alternated. Group A had the MCL ligaments sectioned first, followed by the LCL and AC, sequentially. The elbow was tested in both the overhead and upright supine ROM. Group B had the LCL ligaments sectioned first, followed by the MCL and, sequentially. The experiment protocol is shown in Table 3.1. This was done in an effort to see whether or not this has any affect on the outcome of the testing.

Table 3.1 Experimental Protocol

	Active Motion	Passive Motion
Group A: MCL ligament Severed First	**Specimen 1** Specimen 3 Specimen 5	**Specimen 1** Specimen 3 Specimen 5
Group B: LCL ligament Severed First	**Specimen 2** Specimen 4 Specimen 6	**Specimen 2** Specimen 4 Specimen 6

The stability of the elbow was determined by three factors: elbow joint displacement, internal/external rotation and adduction/abduction. Elbow stability in this study was maximal in the healthy subjects, when all the ligaments were intact. Stability was determined primarily by graphical analysis; determining how well the unstable states of the elbow maintained a pattern and magnitude similar to the stable healthy elbow. To further assist in the analysis, paired two T tests were performed in order to help verify if the results supports the analysis.

3.2 Elbow Joint Displacement

One of the factors used to quantify elbow instability was the change in displacement at the elbow joint. The landmarks used to define the displacement at the elbow were the midpoint between the olecranon and the coronoid process and the medial epicondyle. The intact state of the elbow was defined as the neutral position of the elbow. From the neutral position, the translational changes occurring when the MCL ligament, LCL ligament and AC were severed was computed and evaluated. More importantly, the compression and distraction translations were being computed which was defined as a translation in the z-direction. The change in translational displacement and the standard deviation of these states from the normal were calculated.

3.2.1 Active Motion; Group A

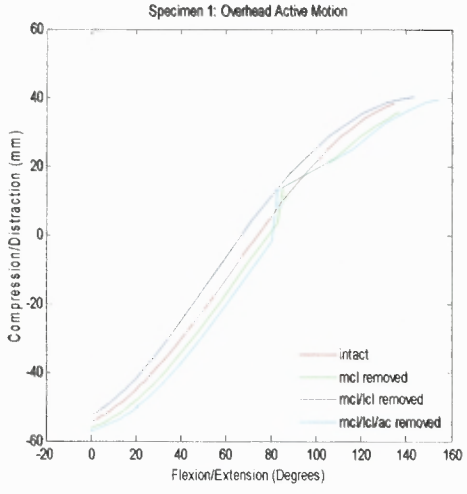

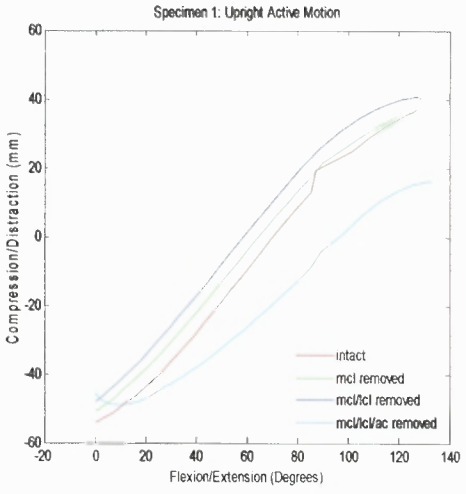

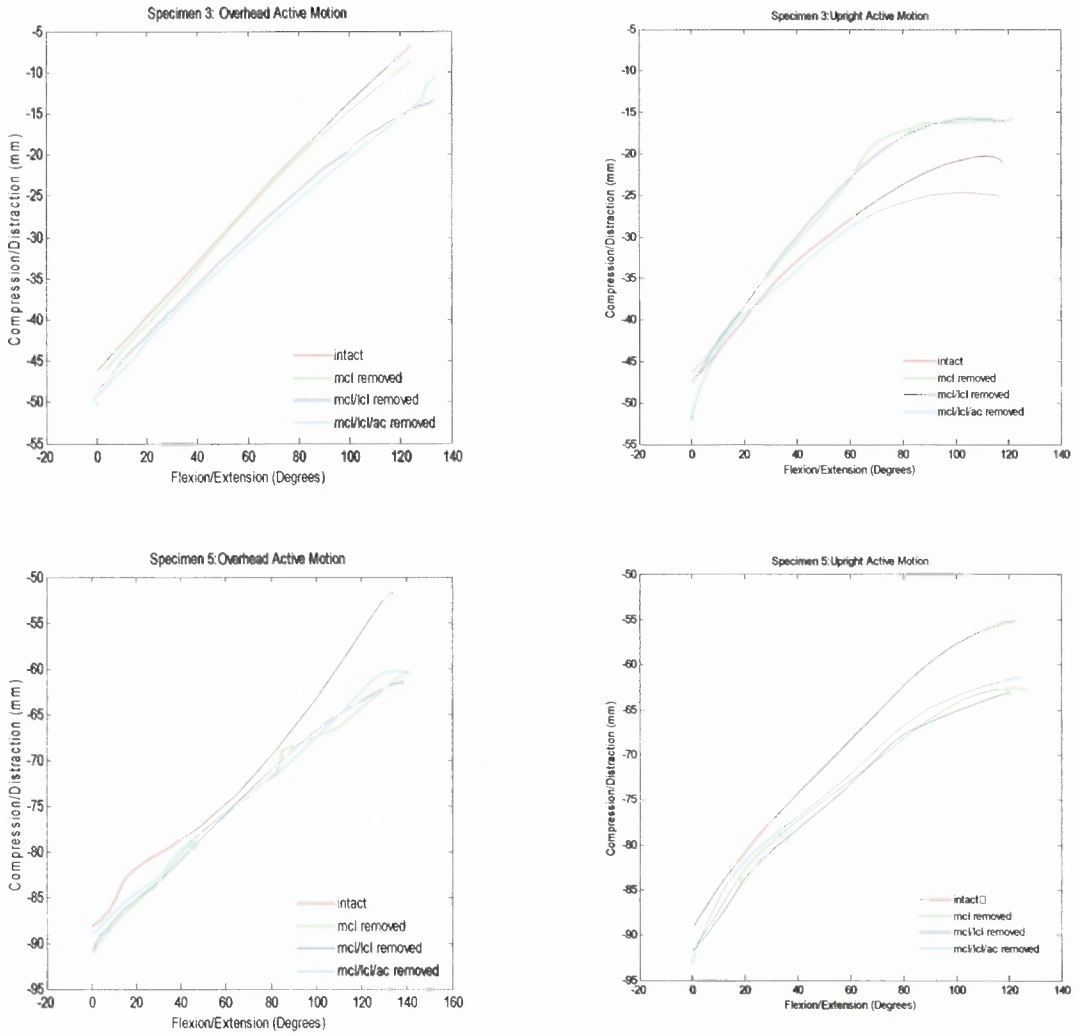

Figure 3.1 Compression and distraction at the elbow joint during active motion when the medial collateral ligament was first severed

Figure 3.1 shows that during active motion, the overhead position showed distraction and compression pattern that was similar and close to that of the normal. These displacement changes during active motion for the overhead protocol and the upright protocol are not large in magnitude. In Specimen one, the overhead ROM distraction and compression changes were not significantly different from the displacement changes occurring in the upright supine ROM ($p>.05$). The same was true for Specimen three ($p>.05$). In Specimen five, the

overhead ROM provided greater stability to the unstable elbow than the upright ROM (p=.003).

3.2.2 Active Motion; Group B

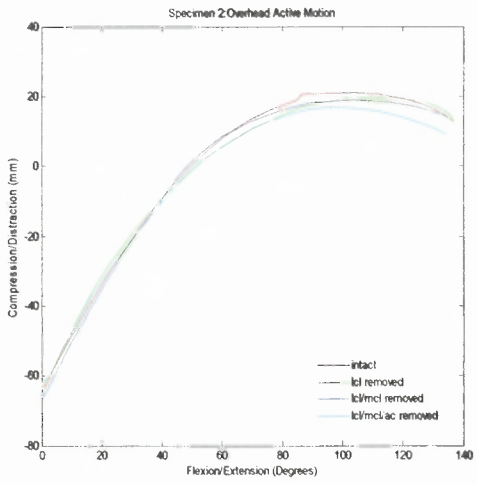

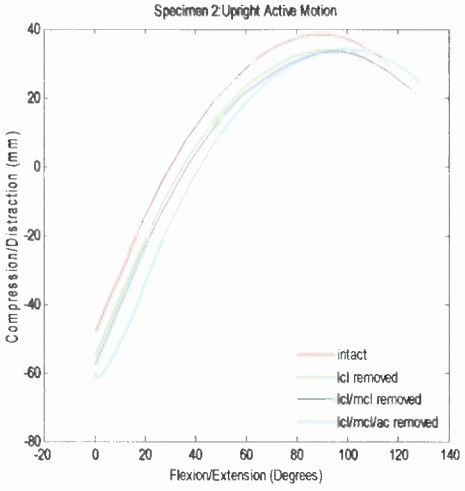

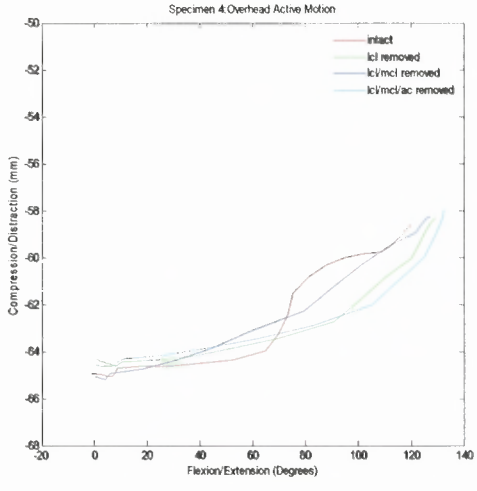

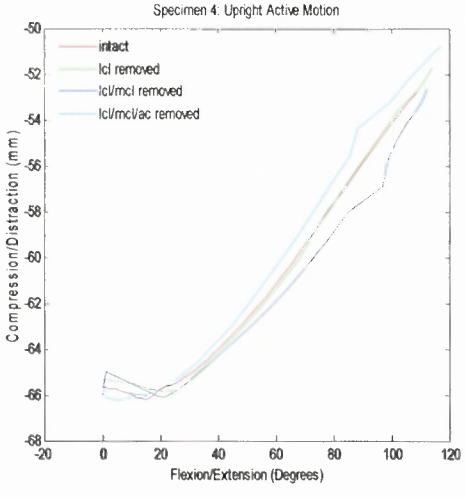

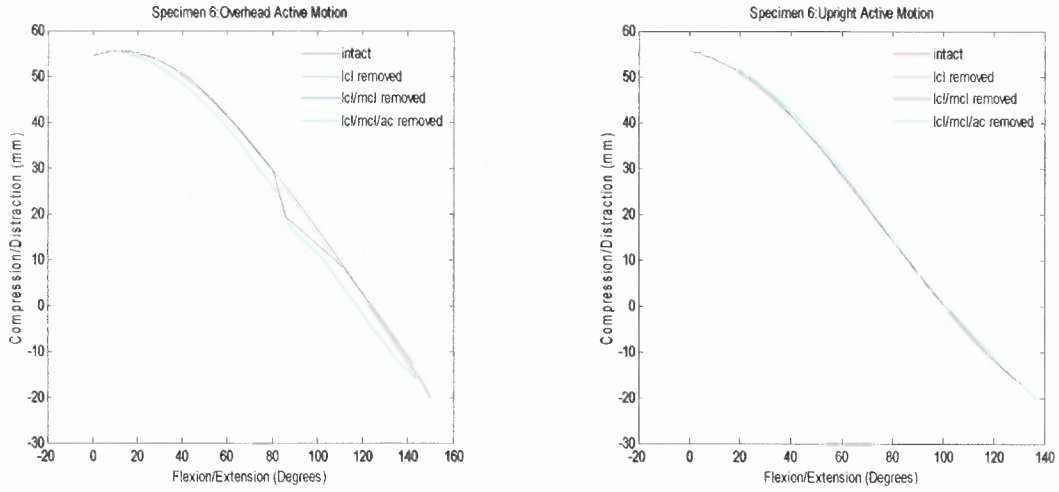

Figure 3.2 Compression and distraction at the elbow joint during active motion when the lateral collateral ligament was first severed

In Figure 3.2, Specimen two showed greater stability in its overhead ROM (p=.005), meanwhile Specimen four (p=0.000) and six (p=.051) maintained a displacement pattern close to the intact elbow's displacement pattern.

3.2.3 Group A; Passive Motion

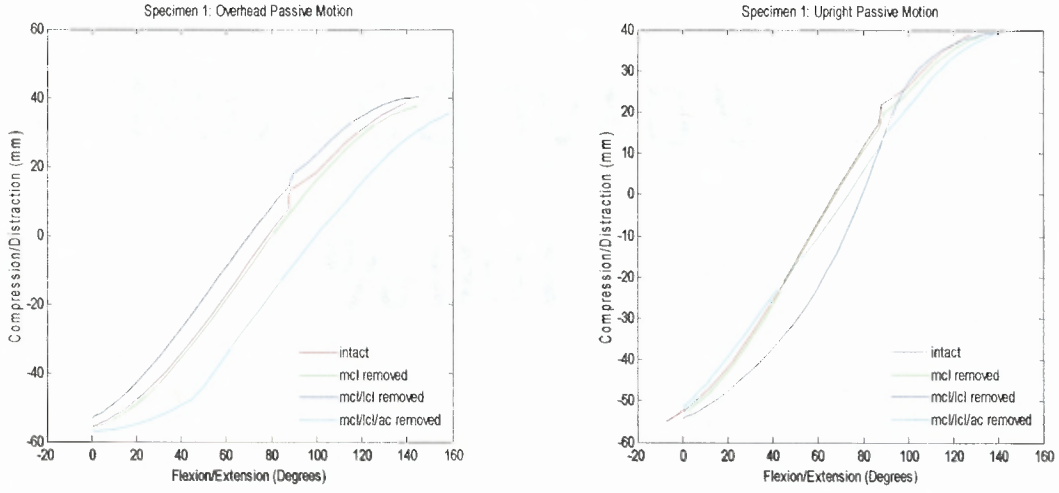

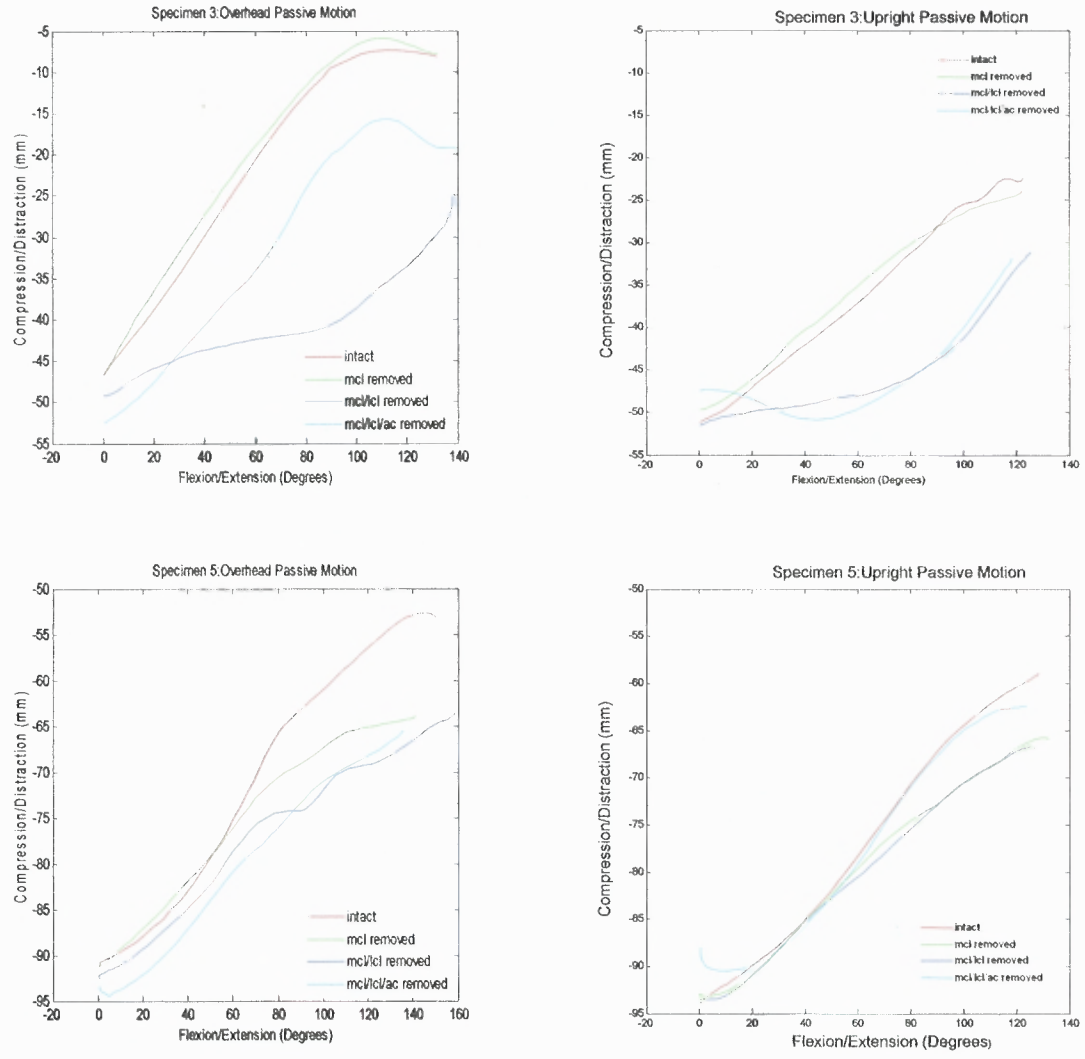

Figure 3.3 Compression and distraction at the elbow joint during passive motion when the medial collateral ligament was first severed

During passive motion, the MCL ligament deficient elbow in its upright ROM, showed greater stability for Group A.

3.2.4 Passive Motion; Group B

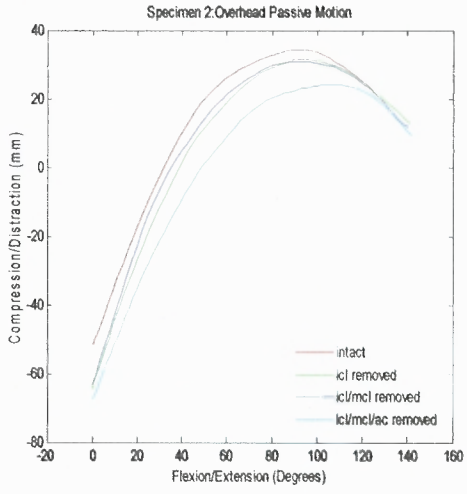

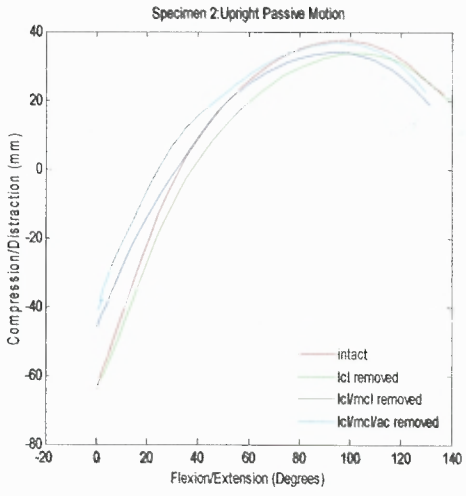

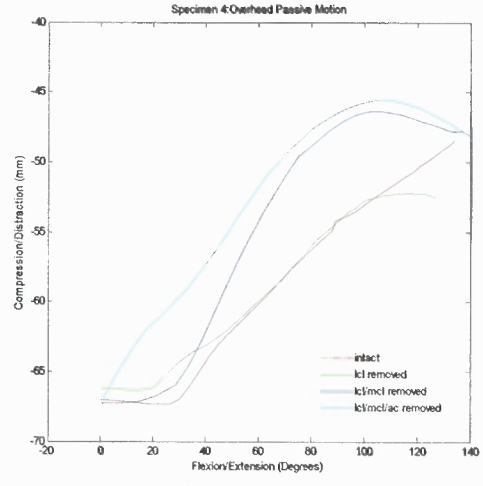

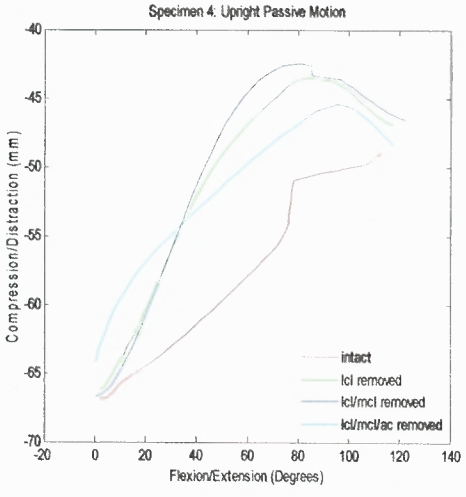

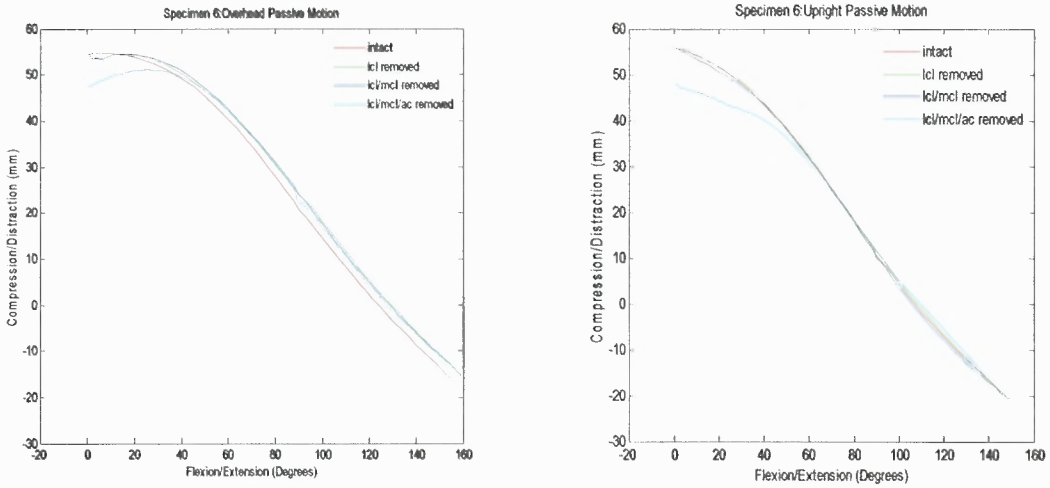

Figure 3.4 Compression and distraction at the elbow joint during passive motion when the lateral collateral ligament was first severed

Specimen two was slightly more stable in the upright ROM than the overhead ROM. In Specimen four, it is difficult to conclude graphically which protocol provided greater stability, but statistically there was no significant difference in stability (p=.225). Specimen six was more stable in the upright ROM because it closely maintained a pattern and magnitude similar to the neutral intact elbow (p=.130).

3.2.5 Standard Deviation; Group A

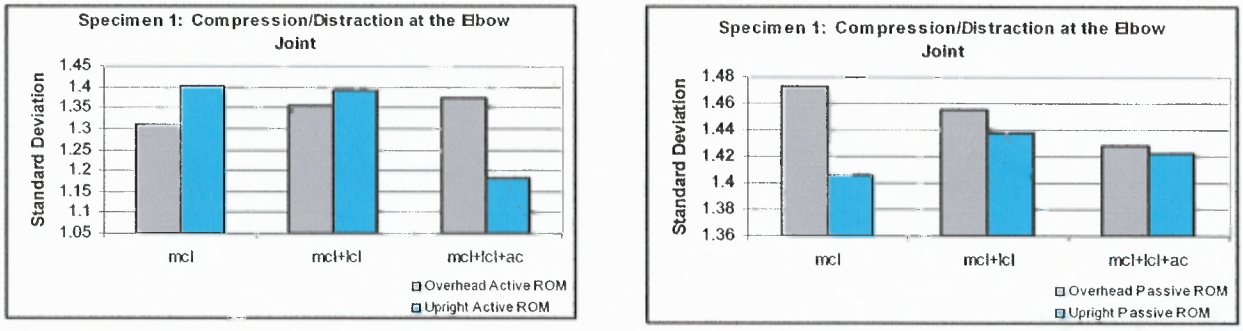

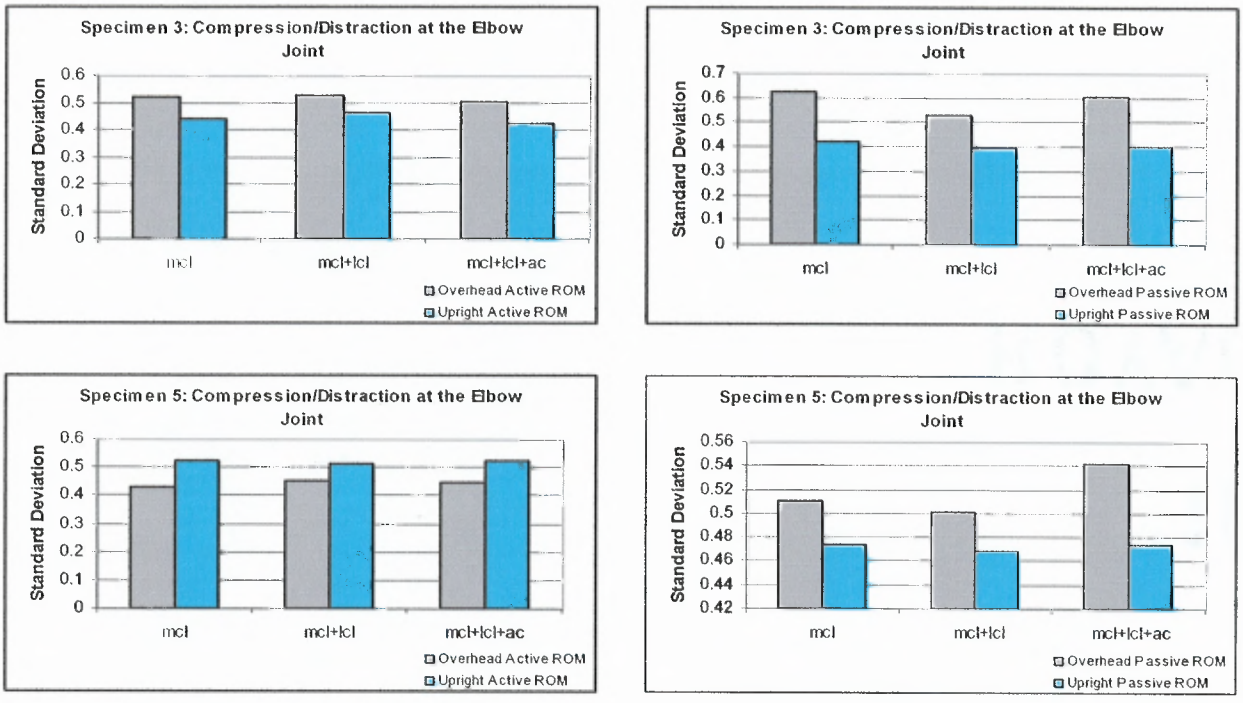

Figure 3.5 The standard deviation of the elbow in its unstable states relative to the healthy intact elbow. This pertains to the set of elbows in which the MCL ligament was first sectioned off.

In Specimen five, the standard deviation for Group A was higher for the upright active ROM than the overhead active ROM for specimen five. Specimen three had a higher standard deviation when positioned in an overhead active ROM. Specimen one during active motion, had variable results; when the MCL was first cut, the upright position had a higher standard deviation. When both the MCL and LCL ligaments were removed, the upright ROM varied greatly from the neutral intact elbow. When all three ligaments were removed, overhead ROM proved to have higher variability than the upright position. Group A during passive motion had a higher standard deviation in the overhead ROM than in its supine upright ROM.

3.2.6 Standard Deviation; Group B

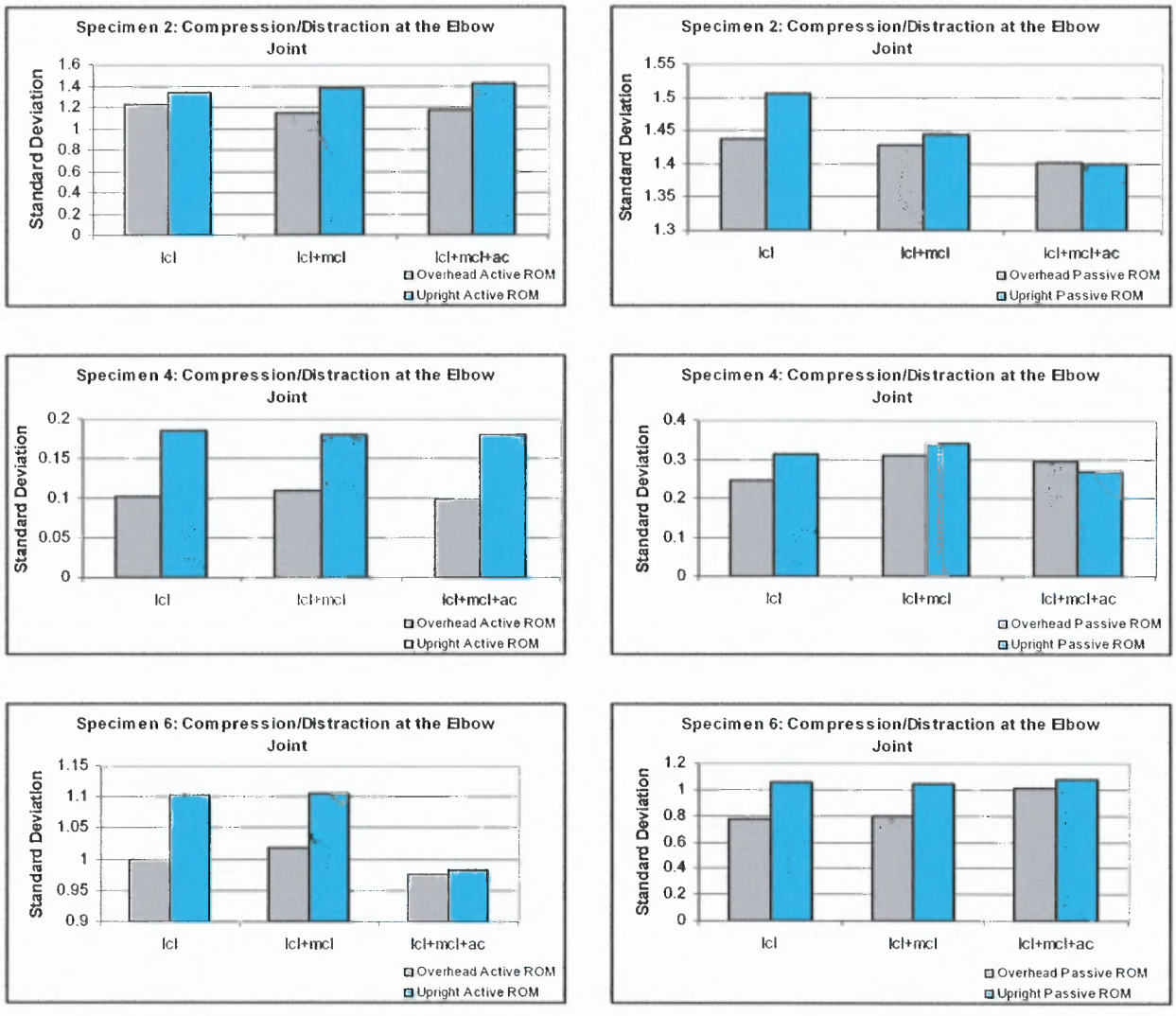

Figure 3.6 The standard deviation of the elbow in its unstable states relative to the healthy intact elbow. This pertains to the set of elbows in which the LCL ligament was first sectioned off.

In Figure 3.6, Group B had higher variability in the upright supine active ROM than in the overhead position. During passive motion, Specimen two and four had higher standard deviation when the 1) LCL ligament 2) LCL and MCL ligaments were removed. In the completely unstable case, Specimen two and Specimen four were slightly less variable in the upright supine passive position. Specimen six was always less variable in the overhead passive ROM.

3.3 Varus/Valgus Instability

Another factor used to describe elbow instability was valgus and varus angulation at the elbow joint. The valgus/varus laxity was computed to determine the level of elbow instability.

3.3.1 Active Motion; Group A

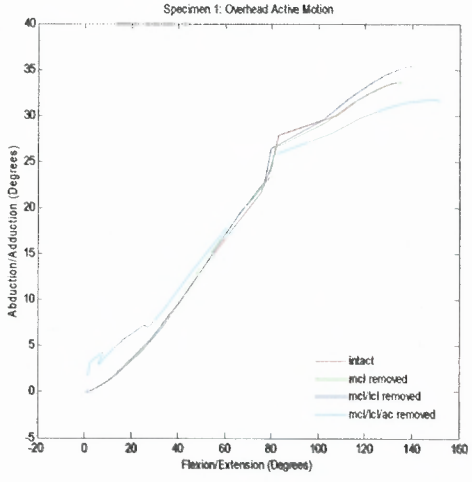

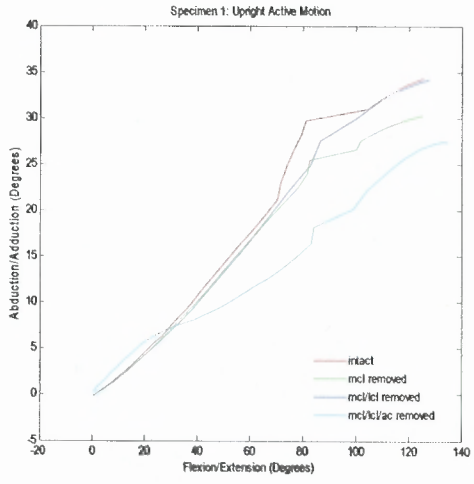

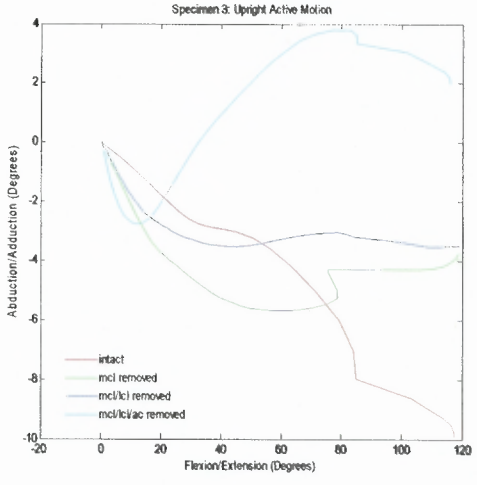

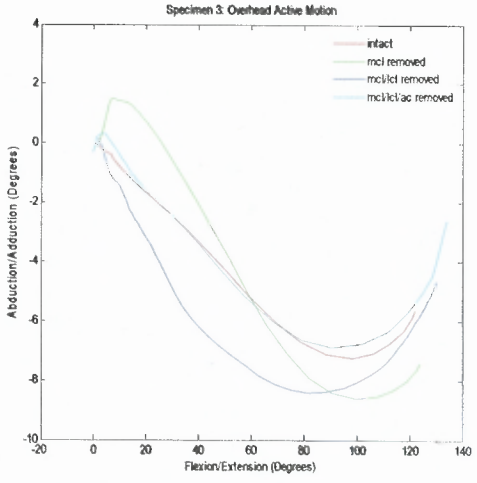

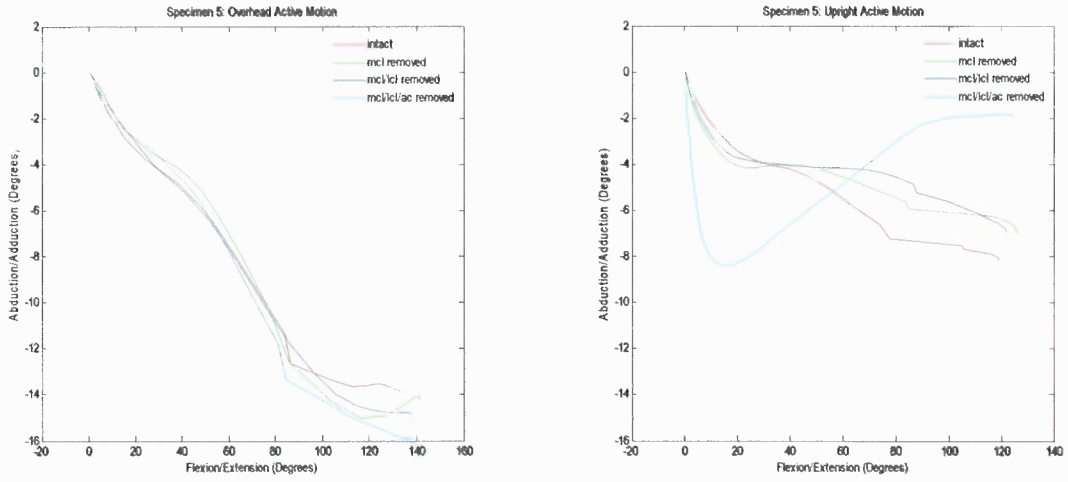

Figure 3.7 Specimen one, three and five's abduction and adduction angles relative to the elbow's flexion and extension angles in its intact and unstable states.

In Figure 3.7 Group A showed greater varus and valgus stability in the overhead ROM than when positioned uprightly. In observing the unstable states of the elbow, the overhead ROM maintains a pattern resembling the intact state and also maintains a closer magnitude to the neutral healthy elbow.

3.3.2 Active Motion; Group B

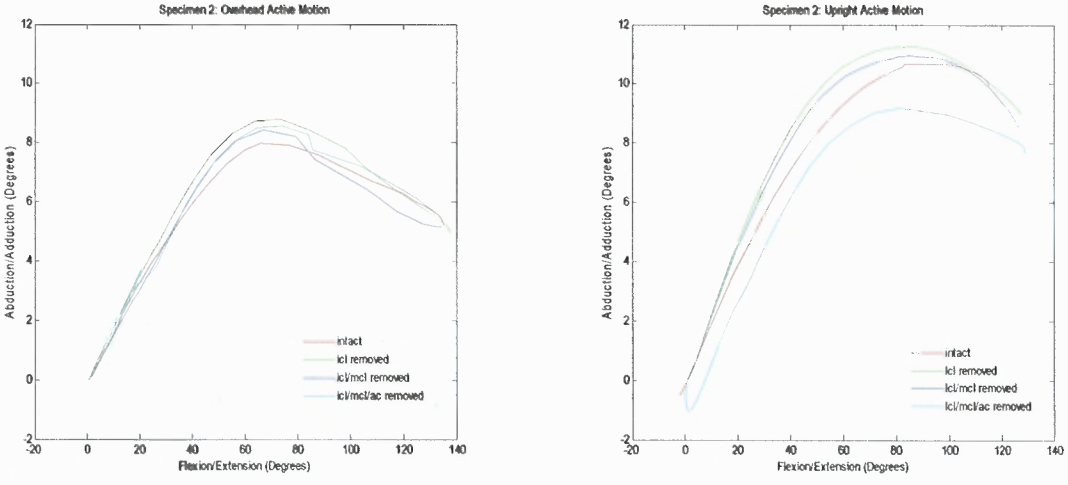

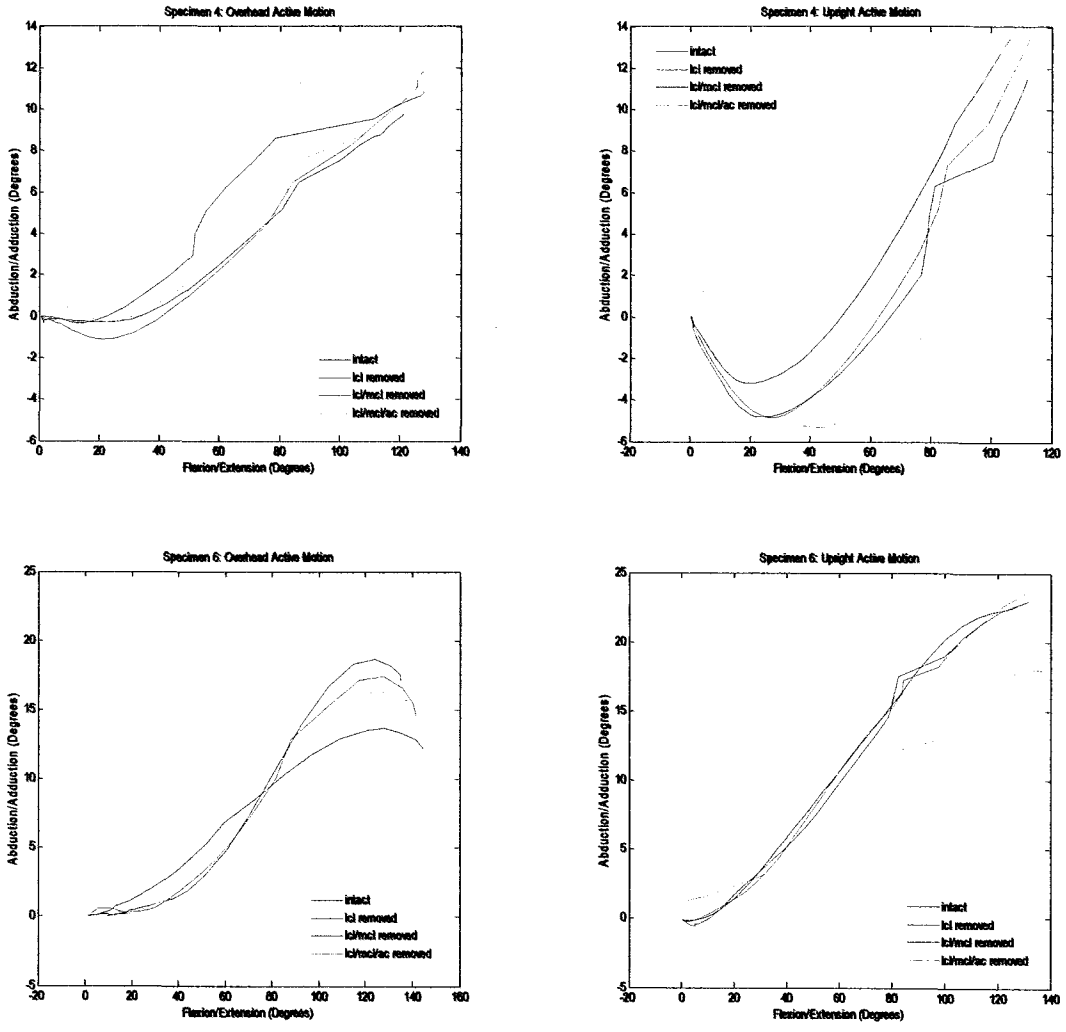

Figure 3.8 Specimen two, four and six's abduction and adduction angles relative to the elbow's flexion and extension angles in its intact and unstable states.

Figure 3.8 shows that Group B show slightly greater stability when placed in an overhead ROM. Specimen two and Specimen six had increased stability in the overhead ROM ($p=.001$, $p=.004$ respectively).

Once the LCL ligament was sectioned, the increase in varus and valgus stability slightly changed when the elbow was placed in the overhead position ($p=.138$). When the MCL ligament was later severed, there was no marked increase in stability for the elbow in its overhead ROM ($p=.192$). In the completely unstable elbow, with all three ligaments

removed, there was not a great effect on stability for the elbow placed in the overhead ROM or placed in the upright ROM (p=.201).

3.3.3 Passive Motion; Group A

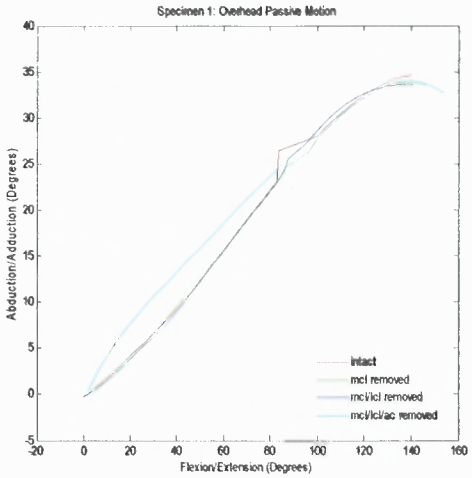

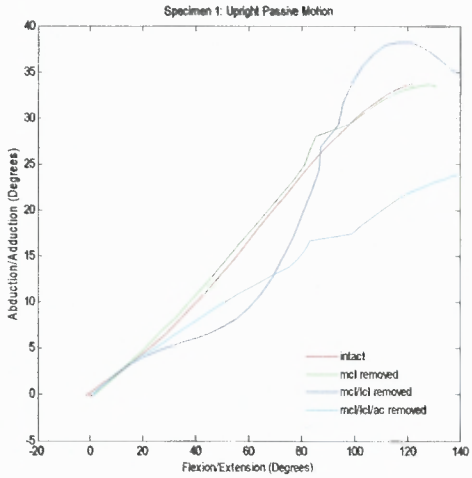

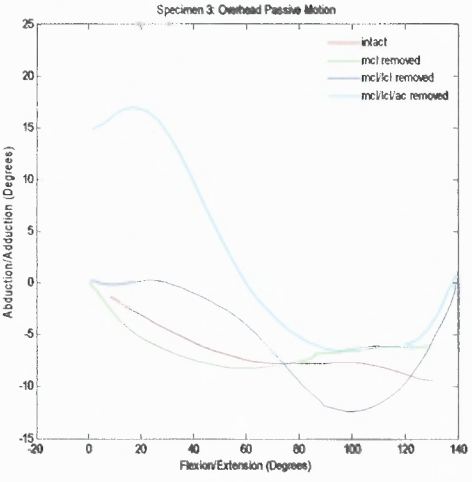

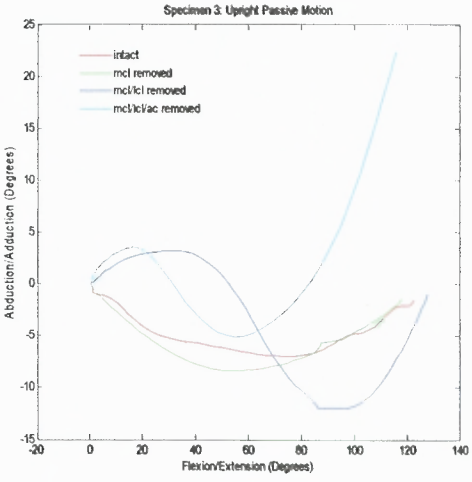

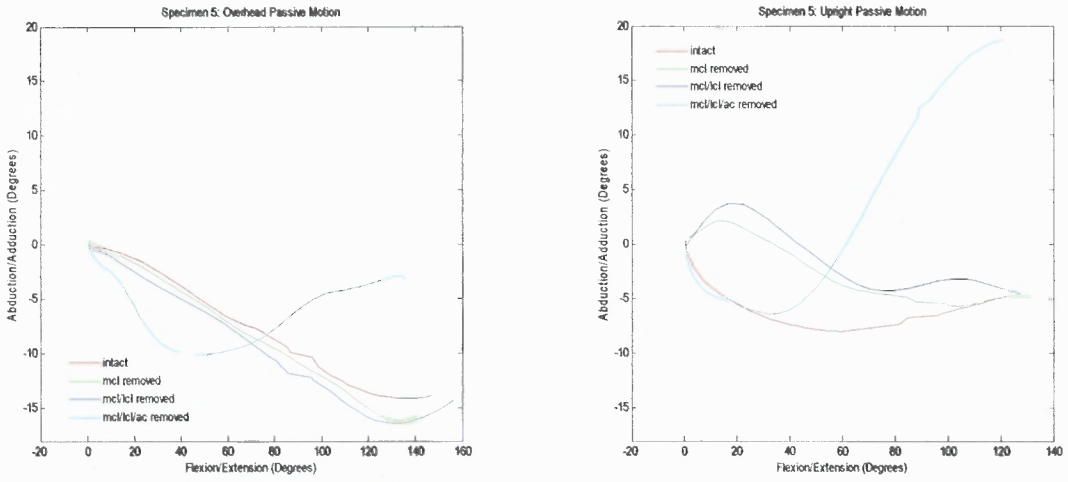

Figure 3.9 Specimen one, three and five's abduction and adduction angles, during passive motion, relative to the elbow's flexion and extension angles in its intact and unstable states.

During passive motion, the abduction and adduction of Group A was more stable in the overhead ROM than in the supine upright ROM.

3.3.4 Passive Motion; Group B

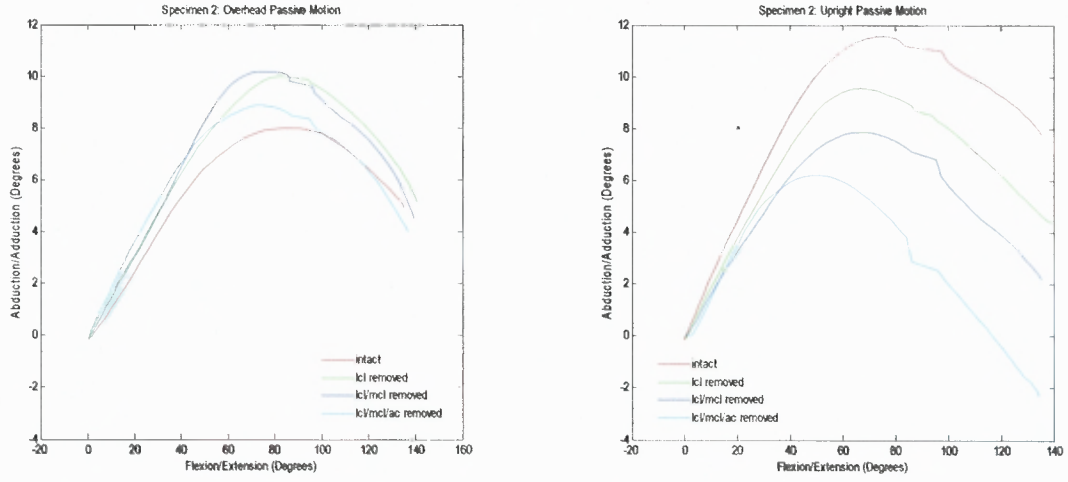

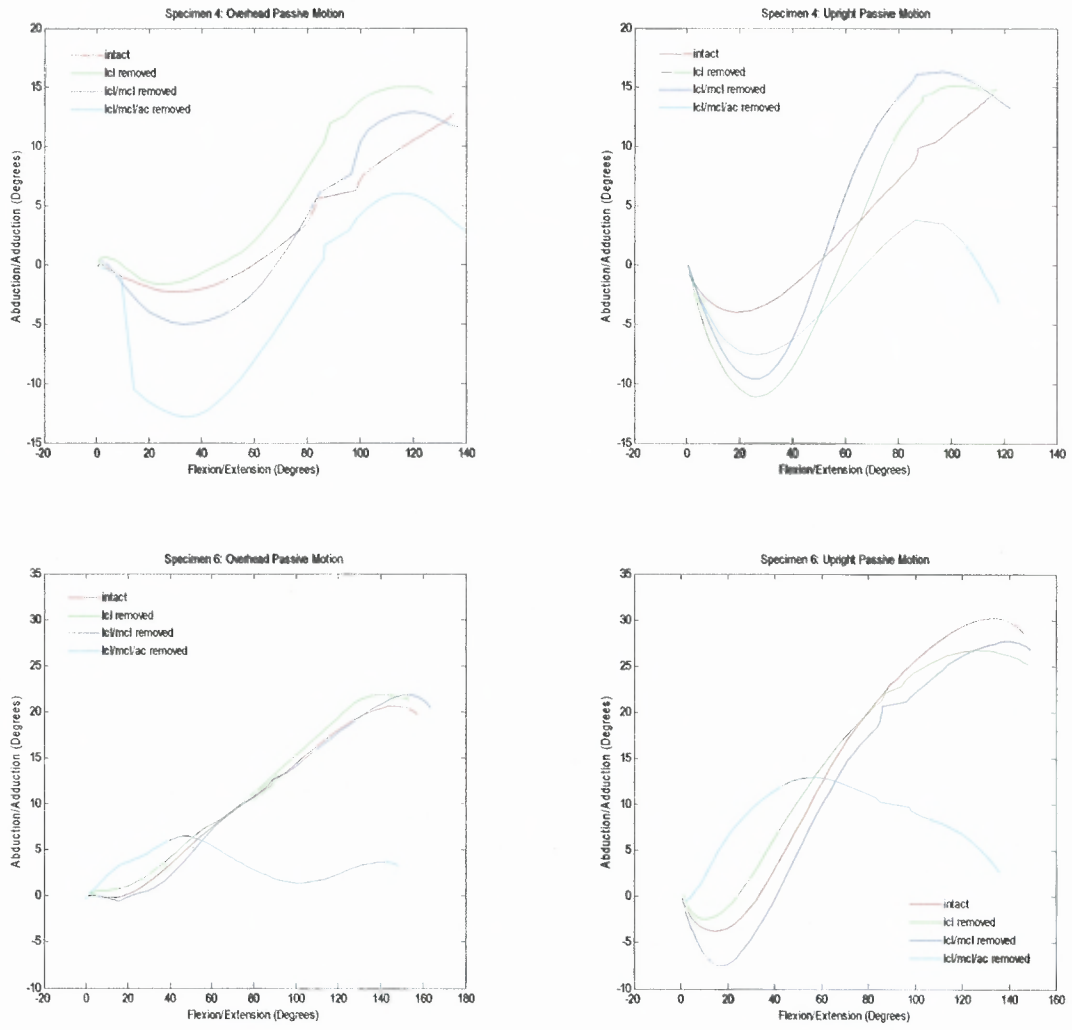

Figure 3.10 Specimen two, four and six's abduction and adduction angles, during passive motion relative to the elbow's flexion and extension angles in its intact and unstable states.

In passive motion, the overhead ROM was more stable than the upright ROM for specimen two and six (p=.007, p=.007). Difficulty was found in graphically interpreting the varus and valgus stability of the elbow in Specimen four relative to both overhead and upright ROM. Statistically, we can conclude that there was not a great difference in stability in the overhead ROM compared to the upright ROM (p=.075).

Statistically, when the LCL, MCL and AC ligaments were sectioned off, there was not a marked increase in stability when placed in an overhead ROM compared to the upright ROM (p=.221, p=.231, p=.243).

3.4 Rotational Instability

The third factor that describes instability is rotational variations, in which the ulna's rotational pattern alters when the MCL, LCL and AC ligaments are cut. The rotational changes from the standard intact state were calculated.

3.4.1 Active Motion; Group A

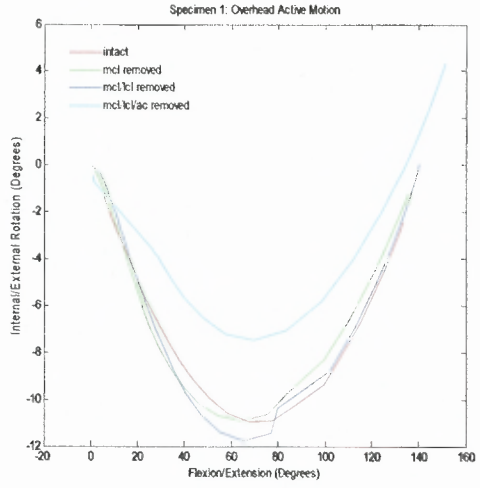

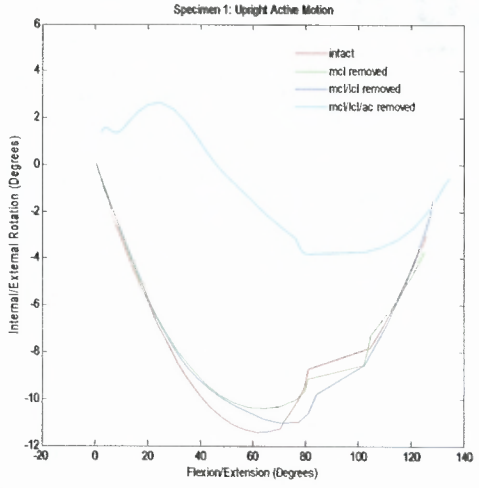

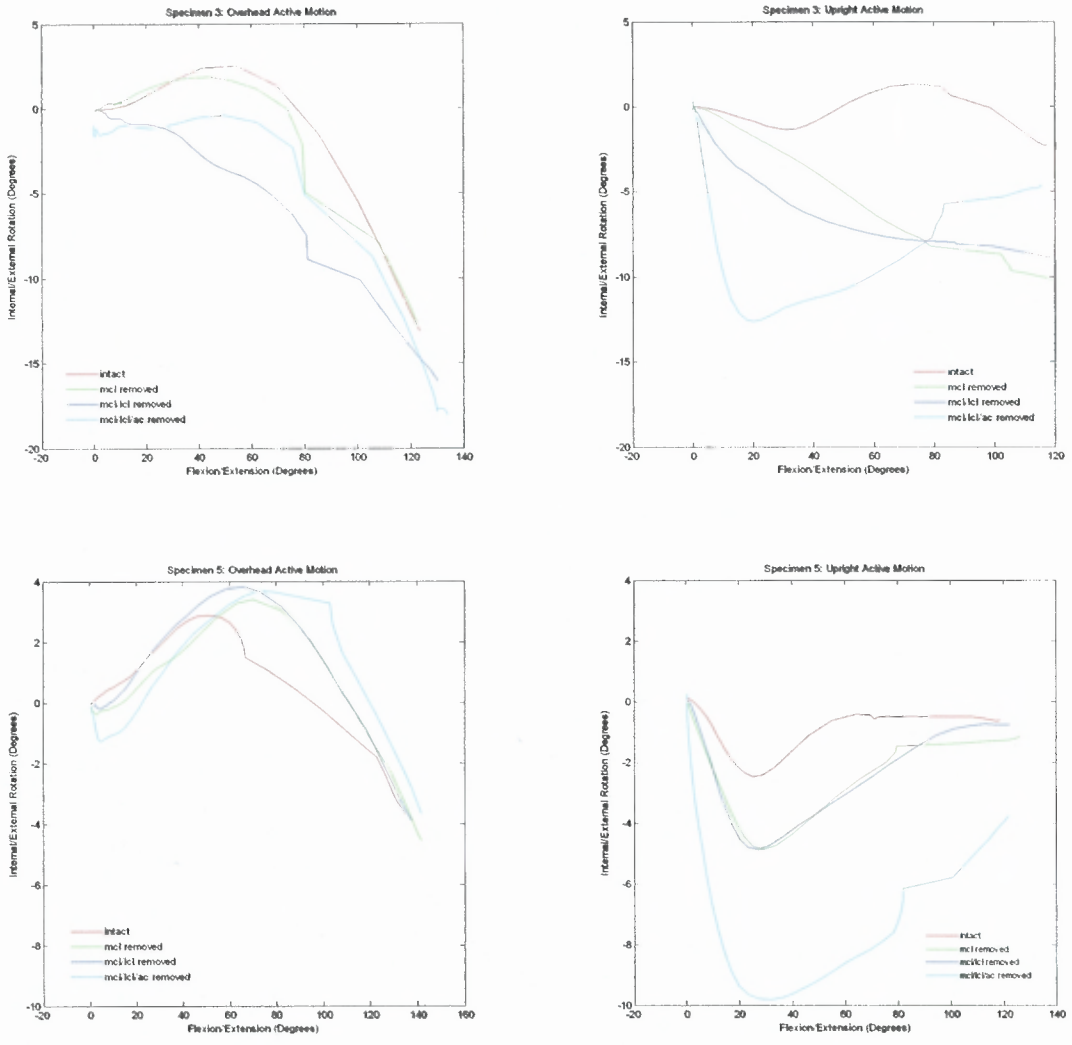

Figure 3.11 Specimen one, three and five's internal and external rotation angles, during active motion, relative to the elbow's flexion and extension angles in its intact and unstable states.

Figure 3.11 shows that the internal and external rotational stability was greater for the overhead active motion of the arm than the upright supine position. For Group A, the overhead position maintained values closer to that of the neutral position. Specimen one maintains greater rotational stability in the overhead active ROM ($p=.006$). Meanwhile the rotational stability of Specimen three, and Specimen five may have been slightly affected by the arm being positioned in the overhead ROM ($p=.932$, $p=.298$, respectively).

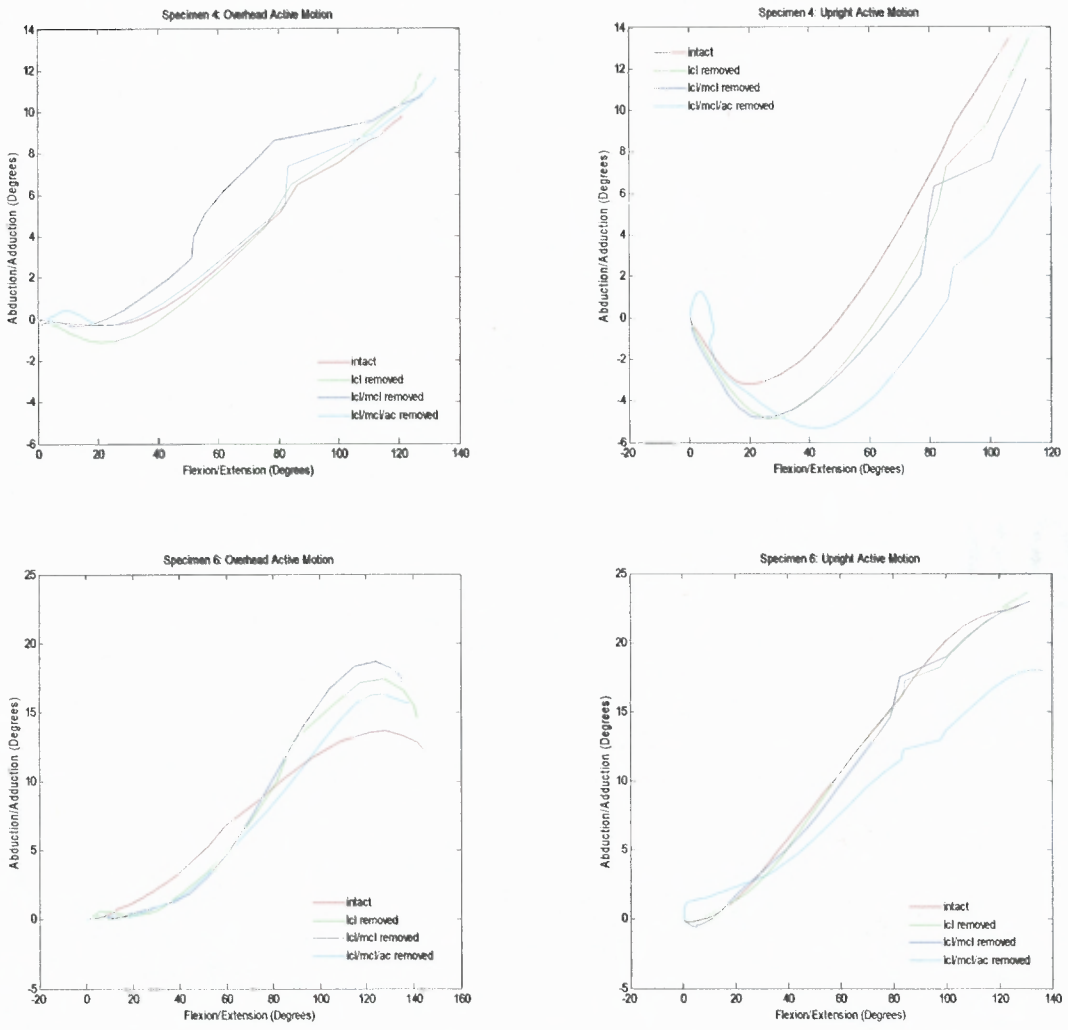

Figure 3.8 Specimen two, four and six's abduction and adduction angles relative to the elbow's flexion and extension angles in its intact and unstable states.

Figure 3.8 shows that Group B show slightly greater stability when placed in an overhead ROM. Specimen two and Specimen six had increased stability in the overhead ROM (p=.001, p=.004 respectively).

Once the LCL ligament was sectioned, the increase in varus and valgus stability slightly changed when the elbow was placed in the overhead position (p=.138). When the MCL ligament was later severed, there was no marked increase in stability for the elbow in its overhead ROM (p=.192). In the completely unstable elbow, with all three ligaments

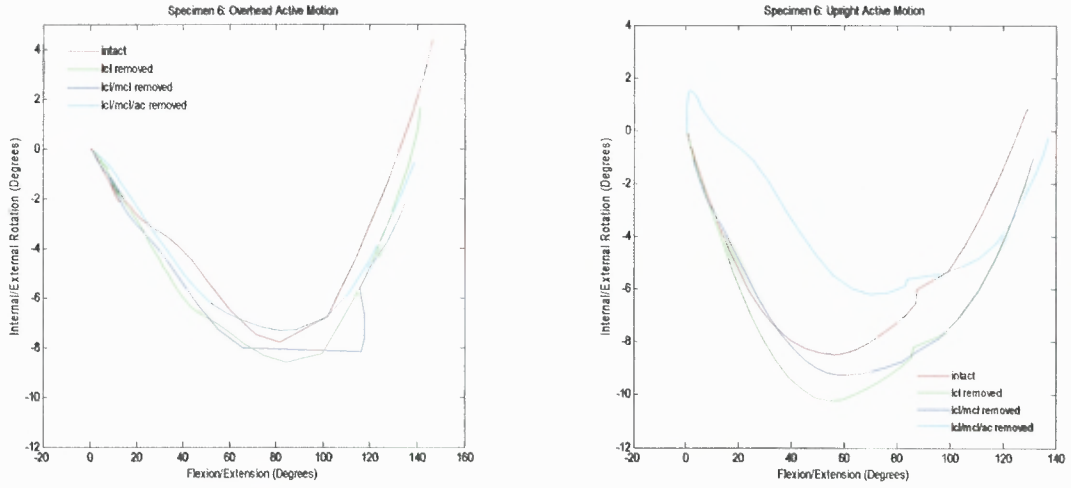

Figure 3.12 Specimen two, four and six's internal and external rotation angles, during active motion, relative to the elbow's flexion and extension angles in its intact and unstable states.

The internal/external rotation of the forearm does not show a consistent trend. Specimen two does not show a gross increase in stability in the overhead ROM (p=.795). In Figure 3.12, Specimen four shows more stability in its overhead ROM than in the supine upright position (p=.014). Specimen six showed more stability in its overhead ROM (p=.007).

3.4.3 Passive Motion; Group A

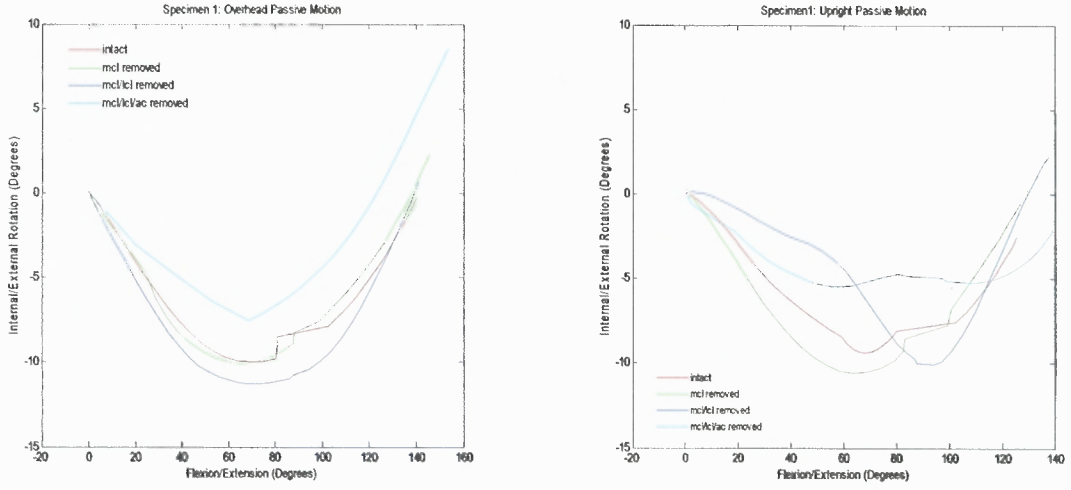

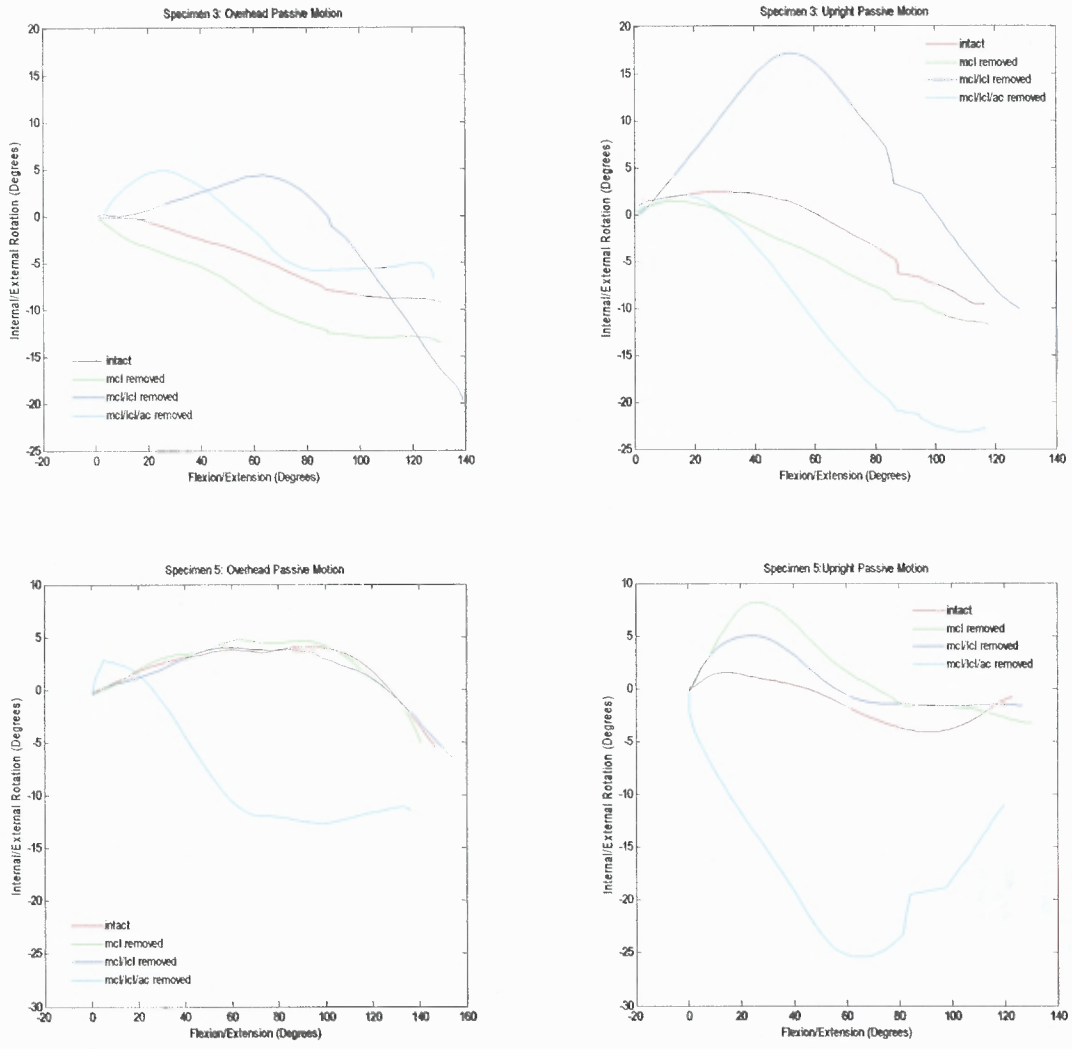

Figure 3.13 Specimen one, three and five's internal and external rotation angles, during passive motion, relative to the elbow's flexion and extension angles in its intact and unstable states.

Graphical analysis indicates that Specimen one and Specimen three showed greater stability in the overhead ROM than in its upright position, during passive motion. Graphically it is shown that Specimen five is more stable in the overhead position because the MCL deficient elbow and the MCL and LCL deficient elbow, better resembled the rotational pattern of the healthy intact elbow. In addition, the magnitude by which the completely unstable elbow differs from the intact elbow was smaller in the overhead ROM than the upright ROM. In regard to the overall change in stability when the each ligament is sectioned off, Specimen

five in the overhead position has an positive affect on stability but not the improvement may not be tremendous (p=.382).

The rotational stability of the elbow remained the slightly unchanged when the MCL ligament was removed (p=.521). The elbow's stability was still not greatly affected when the LCL ligament was removed and when the AC ligament was removed (p=.533, p=.250, respectively).

3.4.4 Passive Motion; Group B

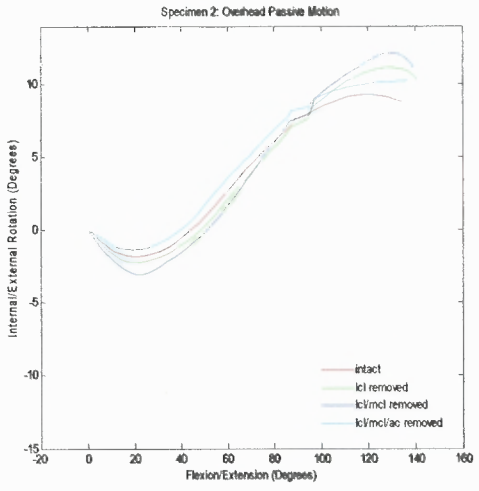

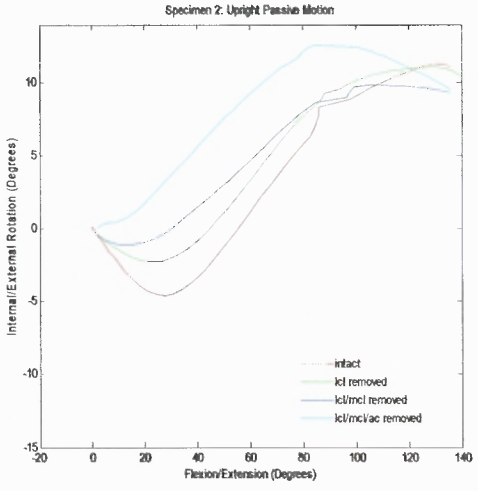

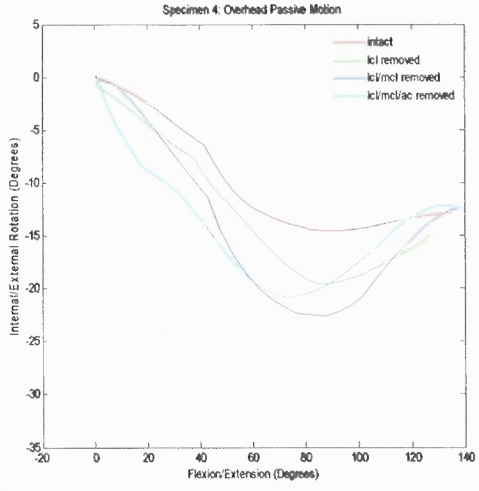

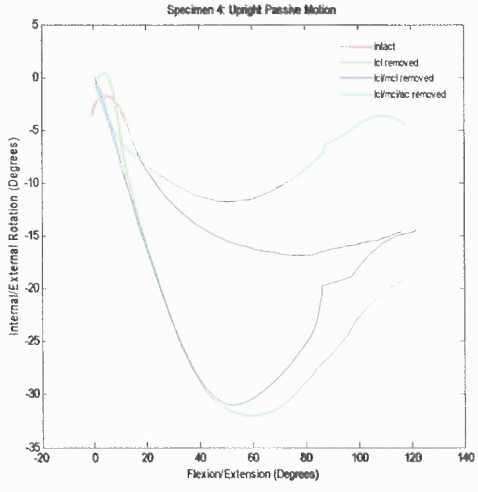

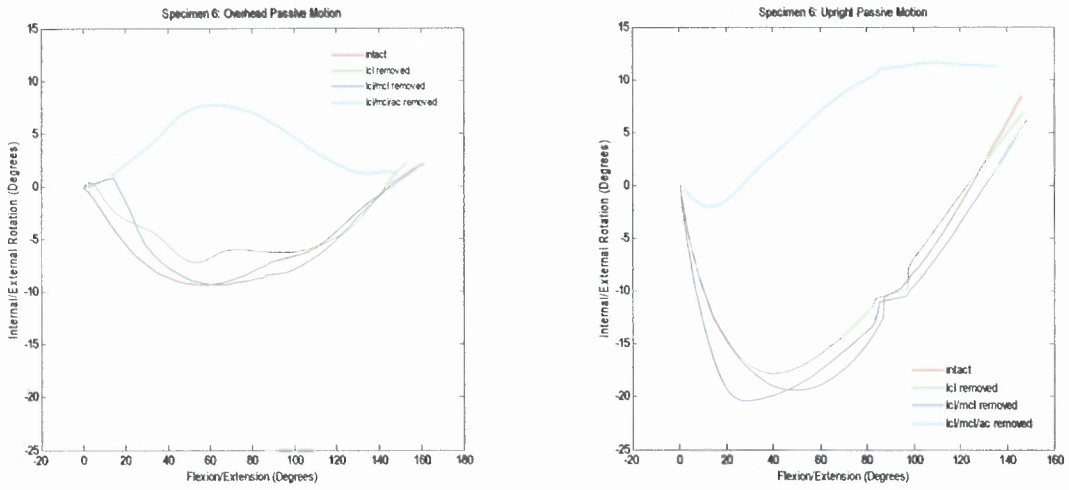

Figure 3.14 Specimen two, four and six's internal and external rotation angles, during passive motion, relative to the elbow's flexion and extension angles in its intact and unstable states.

Figure 3.14 shows that Specimen two provides greater stability during overhead passive ROM than the upright supine position (p=.025). Specimen six was more stable in the overhead ROM because the completely unstable elbow had rotational laxity compared to the upright ROM's rotational laxity (p=.002). Specimen four did not show a marked increase in rotational stability when place through an overhead arc of motion (p=.123).

During overhead ROM in a LCL deficient elbow, rotational stability increased (p=.055). When the MCL ligament and the LCL ligament was removed, the rotational stability did not show a major increase (p=.100, p=.141, respectively).

The level of stability for the elbow, during active motion, irrespective of which ligament was removed, was not largely affected by the fact that the elbow was placed in an overhead ROM. When either the MCL ligament or the LCL ligament was removed the stability was not grossly affected by the positioning of the elbow (p=.272). When both ligaments were sectioned off, the stability remained slightly unaffected by whether or not the elbow was placed in an overhead ROM (p=.526). When all the three ligaments were severed

off, the stability of the elbow was not greatly defined by whether it was placed in an overhead ROM (p=.204).

During passive motion, when either the MCL or the LCL ligament was removed, the rotational stability of the elbow was possibly increased when placed in the overhead ROM (p=.120). When both the MCL and LCL ligaments were sectioned off, the stability of the elbow was not significantly improved in the overhead ROM compared to the upright supine ROM (p=.215). When all three ligaments were removed, the stability may have been improved by the overhead positioning of the arm (p=.077).

CHAPTER 4

DISCUSSION

4.1 Analysis of Elbow Stability

Elbow stability in a healthy elbow is attained with the help from the ligament forces and the muscle tension. The muscles in the elbow joint serve to create compressive forces at the joint. The anatomy of the elbow joint and the joint capsule serve to stabilize the elbow.

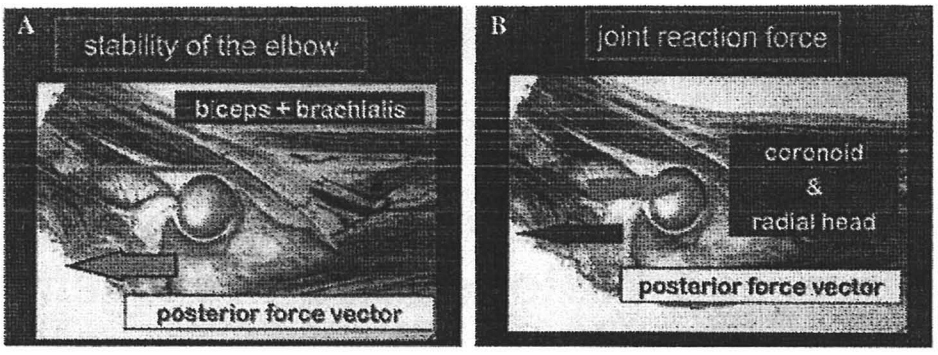

Figure 4.1 The role of the biceps and the brachialis is to provide stability to the elbow and this creates a posterior force vector. The joint reaction force occurs at surfaces such as the coronoid process and the radial head, which also creates a posterior force vector [15].

Elbow stability in this study was maximal in the healthy subjects, when all the ligaments were intact. The condition of the elbow when the MCL, LCL and AC were removed, were compared to the healthy state of the elbow. The varus and valgus rotational changes in the overhead position did offer greater stability at times; maintaining similar rotational patterns to the neutral overhead intact state. This difference in stability was not always consistent, because at times, the upright position offered equivalent, if not, greater stability.

The internal and external rotational stability varied for the six specimens. The overhead ROM offered greater stability for the arm but this notion was not an absolute finding. At times the upright position offered greater stability to the unstable elbow.

Graphically, the overhead ROM helped to maintain a rotational pattern that was similar to the intact healthy elbow 58.3% of the trials, for both passive and active motion. From the analysis of the graphs, the overhead ROM provided greater stability. During active motion, the overhead ROM provided better stability.

The argument can be made that when the elbow is grossly unstable such as in the case when the MCL, LCL and AC are completely disrupted, that no amount of rehabilitation will make the elbow stable. With that notion, the rotational stability, when the MCL and LCL ligaments were removed, during active motion for the most part was increased in the overhead ROM (83.33% of the trials) or equivalent to the stability of the elbow in the supine upright position

When the elbow is in a passive and active ROM, the elbow's varus and valgus stability was more stable when placed in the overhead position. When considering an elbow with incompetent MCL and LCL ligaments, the overhead ROM provided greater stability. During passive motion, the overhead ROM provided greater stability if not equivalent stability to the upright active ROM (83.33%).

It was believed that at the overhead ROM, gravity will serve as a compressive force and decrease the distraction at the elbow joint, but the results did not always support that claim. The distraction and compression at the elbow joint varied for both positions. At times the overhead ROM was more stable than the upright ROM and at times, the upright position served as a greater stabilizer. At times the elbow joint did not distract as much in the upright position and other times the standard deviation of the elbow joint was greater in the overhead ROM. During active motion it was seen graphically that the overhead ROM provided

stability in 50% of the trials. During passive motion, the overhead ROM provided greater stability than the supine upright ROM in 67% of the trials performed.

Elbow joint stability entails several factors including the contact forces between the ulna and the humerus, lateral collateral ligament forces, medial collateral ligament forces, joint reaction forces, the weight of the forearm and gravitational forces. Throughout the range of motion, these forces work in concert to stabilize the elbow, therefore each position yields different reaction forces. In this experiment, the condition of the elbow was altered by first removing the medial collateral ligament, then the lateral collateral ligament and lastly the AC complex. Each time the ligament was removed, different forces were compromised and others had to compensate for the loss of a ligament. In the overhead ROM, the gravitational forces had an effect but it is not certain whether the gravitational force exceeds the other forces at the elbow. It is also not known whether the other forces at the elbow also increase its force to overcome the loss of the ligaments.

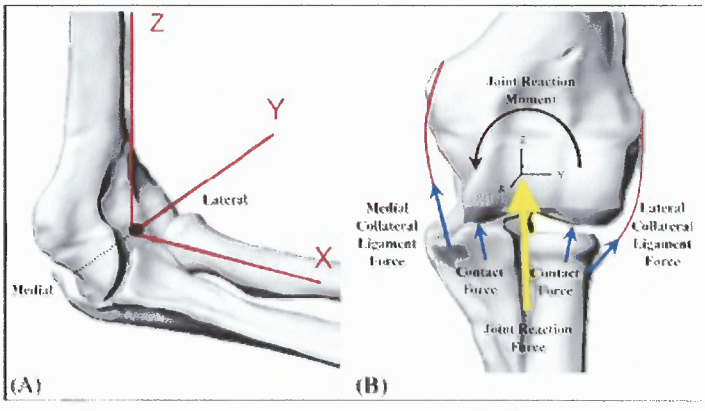

Figure 4.2 The summation of the forces working at the elbow joint in order to maintain stability to the elbow[21].

In the case of the rotational stability and varus/valgus stability the overhead position, for both active and passive ROM provided equal if not better stability than the upright position. In terms of elbow joint distraction and compression, there was not a major

difference in displacement at the joint for the overhead ROM and the supine upright ROM. The statistical analysis did not always support the results of the graph and at times indicated that the differences presented by the positioning of the arm were a result of a random occurrence. Because the statistical analysis is a hypothesis test and it was a secondary source of analysis, its results did not supercede the graphical observation. The graphical analysis provides a better idea of what happens during overhead and upright ROM.

The experiments were performed so that each Specimen either had the MCL ligament cut first or the LCL ligament cut first. There was no correlation between which ligament was sectioned off first and the stability of the elbow. Rotational stability, for the removal of all three ligaments was improved in the overhead ROM for both active and passive motion. When focusing on the stability of a partially unstable elbow (without the removal of the AC ligament), the overhead ROM provided even greater stability to the elbow. Abduction and adduction stability proved increased when in the overhead ROM. It was previously mentioned that the MCL ligament is the primary valgus stabilizer. This was graphically and statistically supported during both active and passive motion.

The difference between the statistical outcome and the graphical analysis can be explained by the magnitude of change in stability. The improvement in stability in most of the cases was relatively small changes. In order to support the claims of the hypothesis, the magnitude by which stability improves needs to be quantified. The question that needs to be answered is whether this improvement in stability will aid in accelerating recuperation and by what factor will stability increase when placed in an overhead ROM.

APPENDIX A

MATLAB SOURCE CODE FOR LANDMARK CALCULATION

```
clear all
%  load the digitization points
load EM
load US
load EL
load RH
load RS
load LT
load US
load CP
load OL

XmmhEM=EM(:,1);
YmmhEM=EM(:,2);
ZmmhEM=EM(:,3);
XaahEM=EM(:,4);
YaahEM=EM(:,5);
ZaahEM=EM(:,6);

%Transformation matrix for flock of birds
XmmhEM=sum(XmmhEM)/(length(XmmhEM))
YmmhEM=sum(YmmhEM)/(length(YmmhEM))
ZmmhEM=sum(ZmmhEM)/(length(ZmmhEM))
XaahEM=sum(XaahEM)/(length(XaahEM))
YaahEM=sum(YaahEM)/(length(YaahEM))
ZaahEM=sum(ZaahEM)/(length(ZaahEM))

% stylus=93.6498
rEM(1,1)=(cosd(YaahEM)*cosd(ZaahEM));
rEM(1,2)=(cosd(YaahEM)*sind(ZaahEM));
rEM(1,3)=-sind(YaahEM);
rEM(2,1)=-cosd(XaahEM)*sind(ZaahEM)+(sind(XaahEM)*sind(YaahEM)*cosd(ZaahEM));
rEM(2,2)=(cosd(XaahEM)*cosd(ZaahEM))+(sind(XaahEM)*sind(YaahEM)*sind(ZaahEM));
rEM(2,3)=sind(XaahEM)*cosd(YaahEM);
rEM(3,1)=(sind(XaahEM)*sind(ZaahEM))+(cosd(XaahEM)*sind(YaahEM)*cosd(ZaahEM));
rEM(3,2)=(sind(XaahEM)*cosd(ZaahEM))+(cosd(XaahEM)*sind(YaahEM)*sind(ZaahEM));
rEM(3,3)=cosd(XaahEM)*cosd(YaahEM)

%Transformation Matrix
ThEM=eye(3,3)
ThEM(1,1)=rEM(1,1)
ThEM(1,2)=rEM(1,2)
```

```
ThEM(1,3)=rEM(1,3)
ThEM(2,1)=rEM(2,1)
ThEM(2,2)=rEM(2,2)
ThEM(2,3)=rEM(2,3)
ThEM(3,1)=rEM(3,1)
ThEM(3,2)=rEM(3,2)
ThEM(3,3)=rEM(3,3)

%Transformation Matrix to calculate the point obtained from the stylus relative to the transmitter
XEM1=XmmhEM+( 0.0984*rEM(1,1))+(0.1969*rEM(2,1))+(stylus*rEM(3,1))
YEM1=YmmhEM+( 0.0984*rEM(1,2))+(0.1969*rEM(2,2))+(stylus*rEM(3,2))
ZEM1=ZmmhEM+( 0.0984*rEM(1,3))+(0.1969*rEM(2,3))+(stylus*rEM(3,3))

EM1=eye(1,3)
EM1(1,1)=XEM1
EM1(1,2)=YEM1
EM1(1,3)=ZEM1
save('EM1')
%%%%%%%%%%%%%%%%%%%%%%%%%%%%%%%%%%%%%%%%%%%%%
XmmhEL=EL(:,1);
YmmhEL=EL(:,2);
ZmmhEL=EL(:,3);
XaahEL=EL(:,4);
YaahEL=EL(:,5);
ZaahEL=EL(:,6);

%Transformation matrix
XmmhEL=sum(XmmhEL)/(length(XmmhEL))
YmmhEL=sum(YmmhEL)/(length(YmmhEL))
ZmmhEL=sum(ZmmhEL)/(length(ZmmhEL))
XaahEL=sum(XaahEL)/(length(XaahEL))
YaahEL=sum(YaahEL)/(length(YaahEL))
ZaahEL=sum(ZaahEL)/(length(ZaahEL))

rEL(1,1)=(cosd(YaahEL)*cosd(ZaahEL));
rEL(1,2)=(cosd(YaahEL)*sind(ZaahEL));
rEL(1,3)=-sind(YaahEL);
rEL(2,1)=-cosd(XaahEL)*sind(ZaahEL)+(sind(XaahEL)*sind(YaahEL)*cosd(ZaahEL));
rEL(2,2)=(cosd(XaahEL)*cosd(ZaahEL))+(sind(XaahEL)*sind(YaahEL)*sind(ZaahEL);
rEL(2,3)=sind(XaahEL)*cosd(YaahEL);
rEL(3,1)=(sind(XaahEL)*sind(ZaahEL))+(cosd(XaahEL)*sind(YaahEL)*cosd(ZaahEL);
rEL(3,2)=(sind(XaahEL)*cosd(ZaahEL))+(cosd(XaahEL)*sind(YaahEL)*sind(ZaahEL);
rEL(3,3)=cosd(XaahEL)*cosd(YaahEL);

%Transformation Matrix
ThEL=eye(3,3)
```

```
ThEL(1,1)=rEL(1,1)
ThEL(1,2)=rEL(1,2)
ThEL(1,3)=rEL(1,3)
ThEL(2,1)=rEL(2,1)
ThEL(2,2)=rEL(2,2)
ThEL(2,3)=rEL(2,3)
ThEL(3,1)=rEL(3,1)
ThEL(3,2)=rEL(3,2)
ThEL(3,3)=rEL(3,3)

%Transformation Matrix to calculate the point obtained from the stylus relative to the transmitter
XEL1=XmmhEL+( 0.0984*rEL(1,1))+(0.1969*rEL(2,1))+(stylus*rEL(3,1))
YEL1=YmmhEL+( 0.0984*rEL(1,2))+(0.1969*rEL(2,2))+(stylus*rEL(3,2))
ZEL1=ZmmhEL+( 0.0984*rEL(1,3))+(0.1969*rEL(2,3))+(stylus*rEL(3,3))

EL1=eye(1,3)
EL1(1,1)=XEL1
EL1(1,2)=YEL1
EL1(1,3)=ZEL1
save('EL1')
%%%%%%%%%%%%%%%%%%%%%%%%%%%%%%%%%%%%%%%%%%%%%%%
XmmhCP=CP(:,1);
YmmhCP=CP(:,2);
ZmmhCP=CP(:,3);
XaahCP=CP(:,4);
YaahCP=CP(:,5);
ZaahCP=CP(:,6);

%Transformation matrix
XmmhCP=sum(XmmhCP)/(length(XmmhCP))
YmmhCP=sum(YmmhCP)/(length(YmmhCP))
ZmmhCP=sum(ZmmhCP)/(length(ZmmhCP))
XaahCP=sum(XaahCP)/(length(XaahCP))
YaahCP=sum(YaahCP)/(length(YaahCP))
ZaahCP=sum(ZaahCP)/(length(ZaahCP))

rCP(1,1)=(cosd(YaahCP)*cosd(ZaahCP));
rCP(1,2)=(cosd(YaahCP)*sind(ZaahCP));
rCP(1,3)=-sind(YaahCP);
rCP(2,1)=-cosd(XaahCP)*sind(ZaahCP)+(sind(XaahCP)*sind(YaahCP)*cosd(ZaahCP));
rCP(2,2)=(cosd(XaahCP)*cosd(ZaahCP))+(sind(XaahCP)*sind(YaahCP)*sind(ZaahCP);
rCP(2,3)=sind(XaahCP)*cosd(YaahCP);
rCP(3,1)=(sind(XaahCP)*sind(ZaahCP))+(cosd(XaahCP)*sind(YaahCP)*cosd(ZaahCP);
rCP(3,2)=(sind(XaahCP)*cosd(ZaahCP))+(cosd(XaahCP)*sind(YaahCP)*sind(ZaahCP);
rCP(3,3)=cosd(XaahCP)*cosd(YaahCP);
```

```
%Transformation Matrix
ThCP=eye(3,3)
ThCP(1,1)=rCP(1,1)
ThCP(1,2)=rCP(1,2)
ThCP(1,3)=rCP(1,3)
ThCP(2,1)=rCP(2,1)
ThCP(2,2)=rCP(2,2)
ThCP(2,3)=rCP(2,3)
ThCP(3,1)=rCP(3,1)
ThCP(3,2)=rCP(3,2)
ThCP(3,3)=rCP(3,3)

%Transformation Matrix to calculate the point obtained from the stylus relative to the transmitter
XCP1=XmmhCP+( 0.0984*rCP(1,1))+(0.1969*rCP(2,1))+(stylus*rCP(3,1))
YCP1=YmmhCP+( 0.0984*rCP(1,2))+(0.1969*rCP(2,2))+(stylus*rCP(3,2))
ZCP1=ZmmhCP+( 0.0984*rCP(1,3))+(0.1969*rCP(2,3))+(stylus*rCP(3,3))

CP1=eye(1,3)
CP1(1,1)=XCP1
CP1(1,2)=YCP1
CP1(1,3)=ZCP1
save('CP1')
%%%%%%%%%%%%%%%%%%%%%%%%%%%%%%%%%%%%%%%%%%%%%%%%
XmmhOL=OL(:,1);
YmmhOL=OL(:,2);
ZmmhOL=OL(:,3);
XaahOL=OL(:,4);
YaahOL=OL(:,5);
ZaahOL=OL(:,6);

%Transformation matrix for flock of birds
XmmhOL=sum(XmmhOL)/(length(XmmhOL))
YmmhOL=sum(YmmhOL)/(length(YmmhOL))
ZmmhOL=sum(ZmmhOL)/(length(ZmmhOL))
XaahOL=sum(XaahOL)/(length(XaahOL))
YaahOL=sum(YaahOL)/(length(YaahOL))
ZaahOL=sum(ZaahOL)/(length(ZaahOL))

rOL(1,1)=(cosd(YaahOL)*cosd(ZaahOL));
rOL(1,2)=(cosd(YaahOL)*sind(ZaahOL));
rOL(1,3)=-sind(YaahOL);
rOL(2,1)=cosd(XaahOL)*sind(ZaahOL)+(sind(XaahOL)*sind(YaahOL)*cosd(ZaahOL);
rOL(2,2)=(cosd(XaahOL)*cosd(ZaahOL))+(sind(XaahOL)*sind(YaahOL)*sind(ZaahOL);
rOL(2,3)=sind(XaahOL)*cosd(YaahOL);
rOL(3,1)=(sind(XaahOL)*sind(ZaahOL))+(cosd(XaahOL)*sind(YaahOL)*cosd(ZaahOL);
rOL(3,2)=(sind(XaahOL)*cosd(ZaahOL))+(cosd(XaahOL)*sind(YaahOL)*sind(ZaahOL);
```

```
rOL(3,3)=cosd(XaahOL)*cosd(YaahOL)

%Transformation Matrix
ThOL=eye(3,3)
ThOL(1,1)=rOL(1,1)
ThOL(1,2)=rOL(1,2)
ThOL(1,3)=rOL(1,3)
ThOL(2,1)=rOL(2,1)
ThOL(2,2)=rOL(2,2)
ThOL(2,3)=rOL(2,3)
ThOL(3,1)=rOL(3,1)
ThOL(3,2)=rOL(3,2)
ThOL(3,3)=rOL(3,3)

%Transformation Matrix to calculate the point obtained from the stylus relative to the transmitter
XOL1=XmmhOL+( 0.0984*rOL(1,1))+(0.1969*rOL(2,1))+(stylus*rOL(3,1))
YOL1=YmmhOL+( 0.0984*rOL(1,2))+(0.1969*rOL(2,2))+(stylus*rOL(3,2))
ZOL1=ZmmhOL+( 0.0984*rOL(1,3))+(0.1969*rOL(2,3))+(stylus*rOL(3,3))

OL1=eye(1,3)
OL1(1,1)=XOL1
OL1(1,2)=YOL1
OL1(1,3)=ZOL1
save('OL1')
%%%%%%%%%%%%%%%%%%%%%%%%%%%%%%%%%%%%%%%%%%%%%%%%%%%%%%%
XmmhRH=RH(:,1);
YmmhRH=RH(:,2);
ZmmhRH=RH(:,3);

XaahRH=RH(:,4);
YaahRH=RH(:,5);
ZaahRH=RH(:,6);

%Transformation matrix
XmmhRH=sum(XmmhRH)/(length(XmmhRH))
YmmhRH=sum(YmmhRH)/(length(YmmhRH))
ZmmhRH=sum(ZmmhRH)/(length(ZmmhRH))
XaahRH=sum(XaahRH)/(length(XaahRH))
YaahRH=sum(YaahRH)/(length(YaahRH))
ZaahRH=sum(ZaahRH)/(length(ZaahRH))

rRH(1,1)=(cosd(YaahRH)*cosd(ZaahRH));
rRH(1,2)=(cosd(YaahRH)*sind(ZaahRH));
rRH(1,3)=-sind(YaahRH);
rRH(2,1)=cosd(XaahRH)*sind(ZaahRH)+(sind(XaahRH)*sind(YaahRH)*cosd(ZaahRH;
rRH(2,2)=(cosd(XaahRH)*cosd(ZaahRH))+(sind(XaahRH)*sind(YaahRH)*sind(ZaahRH));
```

```
rRH(2,3)=sind(XaahRH)*cosd(YaahRH);
rRH(3,1)=(sind(XaahRH)*sind(ZaahRH))+(cosd(XaahRH)*sind(YaahRH)*cosd(ZaahRH));
rRH(3,2)=(-sind(XaahRH)*cosd(ZaahRH))+(cosd(XaahRH)*sind(YaahRH)*sind(ZaahRH));
rRH(3,3)=cosd(XaahRH)*cosd(YaahRH)

%Transformation Matrix
ThRH=eye(3,3)
ThRH(1,1)=rRH(1,1)
ThRH(1,2)=rRH(1,2)
ThRH(1,3)=rRH(1,3)
ThRH(2,1)=rRH(2,1)
ThRH(2,2)=rRH(2,2)
ThRH(2,3)=rRH(2,3)
ThRH(3,1)=rRH(3,1)
ThRH(3,2)=rRH(3,2)
ThRH(3,3)=rRH(3,3)

%Transformation Matrix to calculate the point obtained from the stylus relative to the transmitter
XRH1=XmmhRH+( 0.0984*rRH(1,1))+(0.1969*rRH(2,1))+(stylus*rRH(3,1))
YRH1=YmmhRH+( 0.0984*rRH(1,2))+(0.1969*rRH(2,2))+(stylus*rRH(3,2))
ZRH1=ZmmhRH+( 0.0984*rRH(1,3))+(0.1969*rRH(2,3))+(stylus*rRH(3,3))

RH1=eye(1,3)
RH1(1,1)=XRH1
RH1(1,2)=YRH1
RH1(1,3)=ZRH1
save('RH1')
%%%%%%%%%%%%%%%%%%%%%%%%%%%%%%%%%%%%%%%%%%%%
XmmhRS=RS(:,1);
YmmhRS=RS(:,2);
ZmmhRS=RS(:,3);
XaahRS=RS(:,4);
YaahRS=RS(:,5);
ZaahRS=RS(:,6);

%Transformation matrix
XmmhRS=sum(XmmhRS)/(length(XmmhRS))
YmmhRS=sum(YmmhRS)/(length(YmmhRS))
ZmmhRS=sum(ZmmhRS)/(length(ZmmhRS))
XaahRS=sum(XaahRS)/(length(XaahRS))
YaahRS=sum(YaahRS)/(length(YaahRS))
ZaahRS=sum(ZaahRS)/(length(ZaahRS))

rRS(1,1)=(cosd(YaahRS)*cosd(ZaahRS));
rRS(1,2)=(cosd(YaahRS)*sind(ZaahRS));
rRS(1,3)=-sind(YaahRS);
```

```
rRS(2,1)=-cosd(XaahRS)*sind(ZaahRS)+(sind(XaahRS)*sind(YaahRS)*cosd(ZaahRS));
rRS(2,2)=(cosd(XaahRS)*cosd(ZaahRS))+(sind(XaahRS)*sind(YaahRS)*sind(ZaahRS));
rRS(2,3)=sind(XaahRS)*cosd(YaahRS);
rRS(3,1)=(sind(XaahRS)*sind(ZaahRS))+(cosd(XaahRS)*sind(YaahRS)*cosd(ZaahRS));
rRS(3,2)=(-sind(XaahRS)*cosd(ZaahRS))+(cosd(XaahRS)*sind(YaahRS)*sind(ZaahRS));
rRS(3,3)=cosd(XaahRS)*cosd(YaahRS)

%Transformation Matrix
ThRS=eye(3,3)
ThRS(1,1)=rRS(1,1)
ThRS(1,2)=rRS(1,2)
ThRS(1,3)=rRS(1,3)
ThRS(2,1)=rRS(2,1)
ThRS(2,2)=rRS(2,2)
ThRS(2,3)=rRS(2,3)
ThRS(3,1)=rRS(3,1)
ThRS(3,2)=rRS(3,2)
ThRS(3,3)=rRS(3,3)

%Transformation Matrix to calculate the point obtained from the stylus relative to the transmitter
XRS1=XmmhRS+( 0.0984*rRS(1,1))+(0.1969*rRS(2,1))+(stylus*rRS(3,1))
YRS1=YmmhRS+( 0.0984*rRS(1,2))+(0.1969*rRS(2,2))+(stylus*rRS(3,2))
ZRS1=ZmmhRS+( 0.0984*rRS(1,3))+(0.1969*rRS(2,3))+(stylus*rRS(3,3))

RS1=eye(1,3)
RS1(1,1)=XRS1
RS1(1,2)=YRS1
RS1(1,3)=ZRS1
save('RS1')
%%%%%%%%%%%%%%%%%%%%%%%%%%%%%%%%%%%%%%%%%%%%

XmmhUS=US(:,1);
YmmhUS=US(:,2);
ZmmhUS=US(:,3);
XaahUS=US(:,4);
YaahUS=US(:,5);
ZaahUS=US(:,6);

%Transformation matrix
XmmhUS=sum(XmmhUS)/(length(XmmhUS))
YmmhUS=sum(YmmhUS)/(length(YmmhUS))
ZmmhUS=sum(ZmmhUS)/(length(ZmmhUS))
XaahUS=sum(XaahUS)/(length(XaahUS))
YaahUS=sum(YaahUS)/(length(YaahUS))
ZaahUS=sum(ZaahUS)/(length(ZaahUS))
```

```
rUS(1,1)=(cosd(YaahUS)*cosd(ZaahUS));
rUS(1,2)=(cosd(YaahUS)*sind(ZaahUS));
rUS(1,3)=-sind(YaahUS);
rUS(2,1)=-cosd(XaahUS)*sind(ZaahUS)+(sind(XaahUS)*sind(YaahUS)*cosd(ZaahUS));
rUS(2,2)=(cosd(XaahUS)*cosd(ZaahUS))+(sind(XaahUS)*sind(YaahUS)*sind(ZaahUS));
rUS(2,3)=sind(XaahUS)*cosd(YaahUS);
rUS(3,1)=(sind(XaahUS)*sind(ZaahUS))+(cosd(XaahUS)*sind(YaahUS)*cosd(ZaahUS));
rUS(3,2)=(-sind(XaahUS)*cosd(ZaahUS))+(cosd(XaahUS)*sind(YaahUS)*sind(ZaahUS));
rUS(3,3)=cosd(XaahUS)*cosd(YaahUS)

%Transformation Matrix
ThUS=eye(3,3)
ThUS(1,1)=rUS(1,1)
ThUS(1,2)=rUS(1,2)
ThUS(1,3)=rUS(1,3)
ThUS(2,1)=rUS(2,1)
ThUS(2,2)=rUS(2,2)
ThUS(2,3)=rUS(2,3)
ThUS(3,1)=rUS(3,1)
ThUS(3,2)=rUS(3,2)
ThUS(3,3)=rUS(3,3)

%Transformation Matrix to calculate the point obtained from the stylus relative to the transmitter
XUS1=XmmhUS+( 0.0984*rUS(1,1))+(0.1969*rUS(2,1))+(stylus*rUS(3,1))
YUS1=YmmhUS+( 0.0984*rUS(1,2))+(0.1969*rUS(2,2))+(stylus*rUS(3,2))
ZUS1=ZmmhUS+( 0.0984*rUS(1,3))+(0.1969*rUS(2,3))+(stylus*rUS(3,3))

US1=eye(1,3)
US1(1,1)=XUS1
US1(1,2)=YUS1
US1(1,3)=ZUS1
save('US1')
%%%%%%%%%%%%%%%%%%%%%%%%%%%%%%%%%%%%%%%%%%%

XmmhLT=LT(:,1);
YmmhLT=LT(:,2);
ZmmhLT=LT(:,3);
XaahLT=LT(:,4);
YaahLT=LT(:,5);
ZaahLT=LT(:,6);

%Transformation matrix
XmmhLT=sum(XmmhLT)/(length(XmmhLT))
YmmhLT=sum(YmmhLT)/(length(YmmhLT))
ZmmhLT=sum(ZmmhLT)/(length(ZmmhLT))
XaahLT=sum(XaahLT)/(length(XaahLT))
```

```
YaahLT=sum(YaahLT)/(length(YaahLT))
ZaahLT=sum(ZaahLT)/(length(ZaahLT))

rLT(1,1)=(cosd(YaahLT)*cosd(ZaahLT));
rLT(1,2)=(cosd(YaahLT)*sind(ZaahLT));
rLT(1,3)=-sind(YaahLT);
rLT(2,1)=-cosd(XaahLT)*sind(ZaahLT)+(sind(XaahLT)*sind(YaahLT)*cosd(ZaahLT));
rLT(2,2)=(cosd(XaahLT)*cosd(ZaahLT))+(sind(XaahLT)*sind(YaahLT)*sind(ZaahLT));
rLT(2,3)=sind(XaahLT)*cosd(YaahLT);
rLT(3,1)=(sind(XaahLT)*sind(ZaahLT))+(cosd(XaahLT)*sind(YaahLT)*cosd(ZaahLT));
rLT(3,2)=(-sind(XaahLT)*cosd(ZaahLT))+(cosd(XaahLT)*sind(YaahLT)*sind(ZaahLT));
rLT(3,3)=cosd(XaahLT)*cosd(YaahLT)

%Transformation Matrix
ThLT=eye(3,3)
ThLT(1,1)=rLT(1,1)
ThLT(1,2)=rLT(1,2)
ThLT(1,3)=rLT(1,3)
ThLT(2,1)=rLT(2,1)
ThLT(2,2)=rLT(2,2)
ThLT(2,3)=rLT(2,3)
ThLT(3,1)=rLT(3,1)
ThLT(3,2)=rLT(3,2)
ThLT(3,3)=rLT(3,3)

%Transformation Matrix to calculate the point obtained from the stylus relative to the transmitter
XLT1=XmmhLT+( 0.0984*rLT(1,1))+(0.1969*rLT(2,1))+(stylus*rLT(3,1))
YLT1=YmmhLT+( 0.0984*rLT(1,2))+(0.1969*rLT(2,2))+(stylus*rLT(3,2))
ZLT1=ZmmhLT+( 0.0984*rLT(1,3))+(0.1969*rLT(2,3))+(stylus*rLT(3,3))

LT1=eye(1,3)
LT1(1,1)=XLT1
LT1(1,2)=YLT1
LT1(1,3)=ZLT1
save('LT1')
%%%%%%%%%%%%%%%%%%%%%%%%%%%%%%%%%%%%%%%%%%%%%%%%%%%%%%
XmmhOT=OT(:,1);
YmmhOT=OT(:,2);
ZmmhOT=OT(:,3);
XaahOT=OT(:,4);
YaahOT=OT(:,5);
ZaahOT=OT(:,6);

XmmhOT=sum(XmmhOT)/(length(XmmhOT))
YmmhOT=sum(YmmhOT)/(length(YmmhOT))
ZmmhOT=sum(ZmmhOT)/(length(ZmmhOT))
```

```
XaahOT=sum(XaahOT)/(length(XaahOT))
YaahOT=sum(YaahOT)/(length(YaahOT))
ZaahOT=sum(ZaahOT)/(length(ZaahOT))

rOT(1,1)=(cosd(YaahOT)*cosd(ZaahOT));
rOT(1,2)=(cosd(YaahOT)*sind(ZaahOT));
rOT(1,3)=-sind(YaahOT);
rOT(2,1)=-cosd(XaahOT)*sind(ZaahOT)+(sind(XaahOT)*sind(YaahOT)*cosd(ZaahOT));
rOT(2,2)=(cosd(XaahOT)*cosd(ZaahOT))+(sind(XaahOT)*sind(YaahOT)*sind(ZaahOT));
rOT(2,3)=sind(XaahOT)*cosd(YaahOT);
rOT(3,1)=(sind(XaahOT)*sind(ZaahOT))+(cosd(XaahOT)*sind(YaahOT)*cosd(ZaahOT));
rOT(3,2)=(-sind(XaahOT)*cosd(ZaahOT))+(cosd(XaahOT)*sind(YaahOT)*sind(ZaahOT));
rOT(3,3)=cosd(XaahOT)*cosd(YaahOT)

%Transformation Matrix
ThOT=eye(3,3)
ThOT(1,1)=rOT(1,1)
ThOT(1,2)=rOT(1,2)
ThOT(1,3)=rOT(1,3)
ThOT(2,1)=rOT(2,1)
ThOT(2,2)=rOT(2,2)
ThOT(2,3)=rOT(2,3)
ThOT(3,1)=rOT(3,1)
ThOT(3,2)=rOT(3,2)
ThOT(3,3)=rOT(3,3)

%Transformation Matrix to calculate the point obtained from the stylus relative to the transmitter
XOT1=XmmhOT+( 0.0984*rOT(1,1))+(0.1969*rOT(2,1))+(stylus*rOT(3,1))
YOT1=YmmhOT+( 0.0984*rOT(1,2))+(0.1969*rOT(2,2))+(stylus*rOT(3,2))
ZOT1=ZmmhOT+( 0.0984*rOT(1,3))+(0.1969*rOT(2,3))+(stylus*rOT(3,3))

OT1=eye(1,3)
OT1(1,1)=XOT1
OT1(1,2)=YOT1
OT1(1,3)=ZOT1
save('OT1')
```

APPENDIX B

ROTATION OF THE BONES OF THE FOREARM RELATIVE TO THE HUMERUS

```
clear all;

% Loading the angle data, position data, and time data for both sensors
load ang1xyz.txt;
load ang2xyz.txt;
load position1xyz.txt;
load position2xyz.txt;
load time1.txt

%%%%%%%%%%%%%%%%%%%%%%%%%%%%%%%%%%%%%%%%%%%%%%%%%


% Loading the landmarks of the forearm obtained from the stylus

load US1
load EM1
load EL1
load CP1
load OL1
load OT1
load LT1
load RH1
load RS1

% Landmarks were transformed to get the location of the landmark relative to the transmitter
% US=Ulnar Styloid
% EM=medial epicondyle
% EL=lateral epicondyle
% CP=coronoid process
% OL=olecranon
% OT=mid part of osteotomy, (midshaft)
% LT=Lister's Tubercle
% RH=radial head
% RS=radial styloid


 % The angle data for the sensor on the Ulna and for the sensor on the Radius
Degreenew=[ang1xyz];
Degreenew1=[ang2xyz];
 Degreenew2=[90.62 3.47 12.28]

%%%%%%%%%%%%%%%%%%%%%%%%%%%%%%%%%%%%%%%%%%%%%%%%%
```

```
%Starting Position
for n=1:length(Degreenew)

Xa=Degreenew(:,1);
Ya=Degreenew(:,2);
Za=Degreenew(:,3);

% Filtering Data using a Butterworth Filter for the sensor on the Ulna
[e f]=butter(2,.2);
Xa=filtfilt(e,f,Xa);
Ya=filtfilt(e,f,Ya);
Za=filtfilt(e,f,Za);

% Filtering Data using a Butterworth Filter for the sensor on the Radius
Xb=Degreenew1(:,1);
Yb=Degreenew1(:,2);
Zb=Degreenew1(:,3);
[e1 f1]=butter(2,.2);
Xb=filtfilt(e1,f1,Xb);
Yb=filtfilt(e1,f1,Yb);
Zb=filtfilt(e1,f1,Zb);

% Data from the Humerus
Xc=Degreenew2 (1);
Yc=Degreenew2 (2);
Zc=Degreenew2 (3);

%%%%%%%%%%%%%%%%%%%%%%%%%%%%%%%%%%%%%%%%%%%%%%

% Creating a Rotation Matrix from the Ulna sensor
TM1(1,1,n)=(cosd(Ya(n))*cosd(Za(n)));
TM1(1,2,n)=(cosd(Ya(n))*sind(Za(n)));
TM1(1,3,n)=-sind(Ya(n));

TM1(2,1,n)=-cosd(Xa(n))*sind(Za(n))+(sind(Xa(n))*sind(Ya(n))*cosd(Za(n)));
TM1(2,2,n)=(cosd(Xa(n))*cosd(Za(n)))+(sind(Xa(n))*sind(Ya(n))*sind(Za(n)));
TM1(2,3,n)=sind(Xa(n))*cosd(Ya(n));

TM1(3,1,n)=(sind(Xa(n))*sind(Za(n)))+(cosd(Xa(n))*sind(Ya(n))*cosd(Za(n)));
TM1(3,2,n)=(-sind(Xa(n))*cosd(Za(n)))+(cosd(Xa(n))*sind(Ya(n))*sind(Za(n)));
TM1(3,3,n)=cosd(Xa(n))*cosd(Ya(n));


% Creation of the Rotation Matrix from the Radius sensor
```

```
TS1(1,1,n)=(cosd(Yb(n))*cosd(Zb(n)));
TS1(1,2,n)=(cosd(Yb(n))*sind(Zb(n)));
TS1(1,3,n)=-sind(Yb(n));

TS1(2,1,n)=-cosd(Xb(n))*sind(Zb(n))+(sind(Xb(n))*sind(Yb(n))*cosd(Zb(n)));
TS1(2,2,n)=(cosd(Xb(n))*cosd(Zb(n)))+(sind(Xb(n))*sind(Yb(n))*sind(Zb(n)));
TS1(2,3,n)=sind(Xb(n))*cosd(Yb(n));

TS1(3,1,n)=(sind(Xb(n))*sind(Zb(n)))+(cosd(Xb(n))*sind(Yb(n))*cosd(Zb(n)));
TS1(3,2,n)=(-sind(Xb(n))*cosd(Zb(n)))+(cosd(Xb(n))*sind(Yb(n))*sind(Zb(n)));
TS1(3,3,n)=cosd(Xb(n))*cosd(Yb(n));

% Creation of the Rotation Matrix from the Humerus sensor
TH1(1,1)=(cosd(Yc)*cosd(Zc));
TH1(1,2)=(cosd(Yc)*sind(Zc));
TH1(1,3)=-sind(Yc);

TH1(2,1)=-cosd(Xc)*sind(Zc)+(sind(Xc)*sind(Yc)*cosd(Zc));
TH1(2,2)=(cosd(Xc)*cosd(Zc))+(sind(Xc(n))*sind(Yc)*sind(Zc));
TH1(2,3)=sind(Xc)*cosd(Yc);

TH1(3,1)=(sind(Xc)*sind(Zc))+(cosd(Xc)*sind(Yc)*cosd(Zc));
TH1(3,2)=(-sind(Xc)*cosd(Zc))+(cosd(Xc)*sind(Yc)*sind(Zc));
TH1(3,3)=cosd(Xc)*cosd(Yc);

%%%%%%%%%%%%%%%%%%%%%%%%%%%%%%%%%%%%%%%%%%%%%%%%%%%


% Creating the Ulna Coordinate System
Ulna1(:,:,1)=eye(4,4);
Ulna11(1:3,1)=CP1(1,1:3)'-US1(1,1:3)';
Ulna21=sqrt((Ulna11(1,1)^2)+(Ulna11(2,1)^2)+(Ulna11(3,1)^2));
Ulna1(1,3,1)=(Ulna11(1,1)/Ulna21(1));
Ulna1(2,3,1)=(Ulna11(2,1)/Ulna21(1));
Ulna1(3,3,1)=(Ulna11(3,1)/Ulna21(1));

Ulna111(1:3,1)=cross(Ulna1(1:3,3,1),(CP1(1,1:3,1)'-OL1(1,1:3,1)'));
Ulna211(1)=sqrt((Ulna111(1,1)^2)+(Ulna111(2,1)^2)+(Ulna111(3,1)^2));
Ulna1(1,2,1)=(Ulna111(1,1)/Ulna211(1));
Ulna1(2,2,1)=(Ulna111(2,1)/Ulna211(1));
Ulna1(3,2,1)=(Ulna111(3,1)/Ulna211(1));

Ulna1111(1:3,1)=cross(Ulna1(1:3,3,1),Ulna1(1:3,2,1));
Ulna2111(1)=sqrt((Ulna1111(1,1)^2)+(Ulna1111(2,1)^2)+(Ulna1111(3,1)^2));
Ulna1(1,1,1)=(Ulna1111(1,1)/Ulna2111(1));
Ulna1(2,1,1)=(Ulna1111(2,1)/Ulna2111(1));
Ulna1(3,1,1)=(Ulna1111(3,1)/Ulna2111(1));
```

```
%%%%%%%%%%%%%%%%%%%%%%%%%%%%%%%%%%%%%%%%%%%

 % Creating the Radius Coordinate System
Radius1(:,:,1)=eye(4,4);
Radius11(1:3,1)=RH1(1,1:3,1)'-LT1(1,1:3,1)';
Radius21(1)=sqrt((Radius11(1,1)^2)+(Radius11(2,1)^2)+(Radius11(3,1)^2));
Radius1(1,3,1)=(Radius11(1,1)/Radius21(1));
Radius1(2,3,1)=(Radius11(2,1)/Radius21(1));
Radius1(3,3,1)=(Radius11(3,1)/Radius21(1));

Radius111(1:3,1)=cross(Radius1(1:3,3,1),(RS1(1,1:3,1)'-LT1(1,1:3,1)'));
Radius211(1)=sqrt((Radius111(1,1)^2)+(Radius111(2,1)^2)+(Radius111(3,1)^2));
Radius1(1,2,1)=(Radius111(1,1)/Radius211(1));
Radius1(2,2,1)=(Radius111(2,1)/Radius211(1));
Radius1(3,2,1)=(Radius111(3,1)/Radius211(1));

Radius1111(1:3,1)=cross(Radius1(1:3,3,1),Radius1(1:3,2,1));
Radius2111(1)=sqrt((Radius1111(1,1)^2)+(Radius1111(2,1)^2)+(Radius1111(3,1)^2));
Radius1(1,1,1)=(Radius1111(1,1)/Radius2111(1));
Radius1(2,1,1)=(Radius1111(2,1)/Radius2111(1));
Radius1(3,1,1)=(Radius1111(3,1)/Radius2111(1));

%%%%%%%%%%%%%%%%%%%%%%%%%%%%%%%%%%%%%%%%%%%

 % Transformation of the Data to Obtain the Rotation of the Ulna
newmatrixr(1:3,1:3,n)=(Radius1(1:3,1:3,1))*(TS1(1:3,1:3,n));
newmatrixu(1:3,1:3,n)=(Ulna1(1:3,1:3,1))*(TM1(1:3,1:3,n));
newmatrixh=(1:3,1:3)=Humerus1(1:3,1:3,1)*(TH1(1:3,1:3,1));

% Ulna Relative to Humerus
NEWMATRIX (1:3,1:3,n)=newmatrixu(1:3,1:3,n)*transpose(newmatrixh(1:3,1:3,1));

% Radius Relative to Humerus
newmatrix(1:3,1:3,n)= newmatrixr(1:3,1:3,n)*transpose(newmatrixh(1:3,1:3,1));

%%%%%%%%%%%%%%%%%%%%%%%%%%%%%%%%%%%%%%%%%%%

% Extract and Calculate the Roll, Pitch and Yaw Angles for the Radius
pitchnew(n)=-asin(newmatrix(1,3,n));
pitchnew(n)=real(pitchnew(n));
yawnew(n)=asin(newmatrix(1,2,n)/cos(pitchnew(n)));
yawnew(n)=real(yawnew(n));
rollnew(n)=asin(newmatrix(2,3,n)/cos(pitchnew(n)));
rollnew(n)=real(rollnew(n));
```

```
%%%%%%%%%%%%%%%%%%%%%%%%%%%%%%%%%%%%%%%%%%%%%

% Extract and Calculate the Roll, Pitch and Yaw Angles for the Radius
pitchnew1(n)=-asin(NEWMATRIX(1,3,n));
pitchnew1(n)=real(pitchnew1(n));
yawnew1(n)=asin(NEWMATRIX(1,2,n)/cos(pitchnew1(n)));
yawnew1(n)=real(yawnew1(n));
rollnew1(n)=asin(NEWMATRIX(2,3,n)/cos(pitchnew1(n)));
rollnew1(n)=real(rollnew1(n));

%%%%%%%%%%%%%%%%%%%%%%%%%%%%%%%%%%%%%%%%%%%%%

%Calculate the Displacement Between the Chosen Landmarks
Ulnaposition=[position1xyz];
Humerusposition=[position2xyz];

Ua=Ulnaposition(:,1);
Ub=Ulnaposition(:,2);
Uc=Ulnaposition(:,3);

% Filter Positional Data
[u1 x1]=butter(2,.2);
Ulnaposition(:,1)=filtfilt(u1,x1,Ua);
Ulnaposition(:,2)=filtfilt(u1,x1,Ub);
Ulnaposition(:,3)=filtfilt(u1,x1,Uc);

% 4x4 Matrix of the Sensor on the Radius
TM1new(1,1,n)=TM1(1,1,n);
TM1new(1,2,n)=TM1(1,2,n);
TM1new(1,3,n)=TM1(1,3,n);
TM1new(1,4,n)=Ulnaposition(n,1)';
TM1new(2,1,n)=TM1(2,1,n);
TM1new(2,2,n)=TM1(2,2,n);
TM1new(2,3,n)=TM1(2,3,n);
TM1new(2,4,n)=Ulnaposition(n,2)';
TM1new(3,1,n)=TM1(3,1,n);
TM1new(3,2,n)=TM1(3,2,n);
TM1new(3,3,n)=TM1(3,3,n);
TM1new(3,4,n)=Ulnaposition(n,3)';
TM1new(4,1,n)=0;
TM1new(4,2,n)=0;
TM1new(4,3,n)=0;
TM1new(4,4,n)=1;
```

```
% Obtain the Landmarks Relative to the Ulna Sensor
OLnew(1:4,n)=(inv(TM1new(1:4,1:4,n))*[OL1 1]');
CPnew(1:4,n)=(inv(TM1new(1:4,1:4,n))*[CP1 1]');
ELnew(1:4,n)=(inv(TM1new(1:4,1:4,n))*[EL1 1]');
EMnew(1:4,n)=(inv(TM1new(1:4,1:4,n))*[EM1 1]');
OTnew(1:4,n)=(inv(TM1new(1:4,1:4,n))*[OT1 1]');
USnew(1:4,n)=(inv(TM1new(1:4,1:4,n))*[US1 1]');
RHnew(1:4,n)=(inv(TM1new(1:4,1:4,n))*[RH1 1]');

 % Calculation of the distraction and compression at the midpoint of the ulna from the medial
epicondyle

 distractvarus(1:3,n)=((CPnew(1:3,n)+OLnew(1:3,n))/2)-(EMnew(1:3,n));

end

%%%%%%%%%%%%%%%%%%%%%%%%%%%%%%%%%%%%%%%%%%%%%%%%%%%%%%%%%%%%%%%%%%%%%%%%%%%%%%%%%%%%%%%%%%%%%%%
```

APPENDIX C

C++ VISUAL BASIC CODE USED TO EXTRACT DATA FROM THE WINBIRD

```
#include <iostream>
#include <fstream>
#include <strstream>

using namespace std;

int main()
{
	ifstream infile("text2.txt", ios::in);
	ofstream outfile("write2.txt", ios::out);

	char a[40], b[40], c[40], d[40], e[40], f[40], g[40], h[40], i[40];
	char j[40], k[40], l[40], m[40], n[40], o[40], p[40], q[40], r[40], s[40], t[40];

	while (!infile.eof())
	{
		infile >> a >> b >> c >> d >> e >> f >> g >> h >> i >> j >> k >> l >> m >> n
>> o;
	//	cout << a <<"\t" << b <<"\t" << c <<"\t" << d <<"\t" << e <<"\t" << f <<"\t";
	//	cout << g <<"\t" << h <<"\t" << i <<"\t" << j <<"\t" << k <<"\t" << l <<"\t"
<< endl;

		a[4]='\t';
		d[4]='\t';
		g[5]='\t';
		h[4]='\t';
		k[4]='\t';
		n[5]='\t';

		outfile << a <<"\t" << b <<"\t" << c <<"\t" << d <<"\t" << e <<"\t" << f
<<"\t";
		outfile << g <<"\t" << h <<"\t" << i <<"\t" << j <<"\t" << k <<"\t" << l <<"\t";
		outfile << m <<"\t" << n << endl;
	}

	infile.close();
	outfile.close();

	ifstream outfile2("write2.txt", ios::in);
	ofstream outfile3("write3.txt", ios::out);
	ofstream pos1("position1xyz.txt", ios::out);
	ofstream pos2("position2xyz.txt", ios::out);
```

```
	ofstream ang1("ang1xyz.txt", ios::out);
	ofstream ang2("ang2xyz.txt", ios::out);
	ofstream time1("time1.txt", ios::out);
	ofstream time2("time2.txt", ios::out);


	outfile3 << "1posX" <<"\t" << "1posY" <<"\t" << "1posZ" <<"\t" << "1angX" <<"\t"
<< "1angY" <<"\t" << "1angZ" << "\t";
	outfile3 << "1time" <<"\t";
	outfile3 << "2posX" <<"\t" << "2posY" <<"\t" << "2posZ" <<"\t" << "2angX" <<"\t"
<< "2angY" <<"\t" << "2angZ" << "\t";
	outfile3 << "2time" << endl;
	while (outfile2 >> a >> b >> c >> d >> e >> f >> g >> h >> i >> j >> k >> l >> m >>
n >> o >> p >> q >> r >> s >> t)
	{
		outfile3 << b <<"\t" << c <<"\t" << d <<"\t" << f <<"\t";
		outfile3 << g <<"\t" << h <<"\t" << j <<"\t" << k <<"\t" << l <<"\t";
		outfile3 << n <<"\t" << o <<"\t" << p << "\t" << q << "\t";
		outfile3 << r <<"\t" <<"\t" << t << endl;

		pos1 << b <<"\t" << c <<"\t" << d << endl;
		ang1 << f <<"\t" << g <<"\t" << h << endl;
		pos2 << l <<"\t" << m <<"\t" << n << endl;
		ang2 << p <<"\t" << q <<"\t" << r << endl;
		time1 << j << endl;
		time2 << t << endl;

	}

	cout << "file finished processing" << endl;

	outfile2.close();
	outfile3.close();
	pos1.close();
	pos2.close();
	ang1.close();
	ang2.close();


	system("pause");

	return 0;
}
```

REFERENCES

1. Armstrong, A.D., Dunning, C.E., Faber, K.J., Duck, T.R., Johnson, J.A., & King, G.J.W. (2000). Rehabilitation of the medial collateral ligament-deficient elbow: An in vitro biomechanical study. The Journal of Hand Surgery, 25A (6), 1051-1056.

2. Dunning, C.E., Zarzour Z.D.S., Patterson, S.D., Johnson, J.A., & King, G.J.W. (2001). Ligamentous stabilizers against posterolateral rotatory instability of the elbow. The Journal of Bone and Joint Surgery, Incorporated, 83-A (12), 1823-1828.

3. Kamineni, S., Hirahara, H., Pomianowski, S., Neale, P.G., O'Driscoll, S.W., Elattrache, N., An, K.N., & Morrey, B.F. (2003). Partial posteromedial olecranon resection: A kinematic study. The Journal of Bone and Joint Surgery, Incorporated, 85-A (6), 1005-1011.

4. Cain, E.L. Jr., Dugas, J.R., Wolf, R.S., & Andrews, J.R. (2003). Elbow injuries in throwing athletes: A current concepts review. American Journal of Sports Medicine, 31 (4), 621-635.

5. An, K. N., Jacobsen, C., Berglund, L.J., & Chao, Y.S. (1988). Application of magnetic tracking device to kinesiologic studies. Journal of Biomechanics, 21 (7), 613 – 620.

6. Bull, A.M.J., Berkshire, F.H., & Amis, A.A. (1998). Accuracy of an electromagnetic measurement device and application to the measurement and description of knee joint motion. Proceeding of the Institution of Mechanical Engineers, 212 (H), 347-355.

7. Ying, N., & Kim, W. Determining dual Euler angles of the ankle complex in vivo using "flock of birds" electromagnetic tracking device. 127. Retrieved August 10, 2007, from http//www.asme.org/terms/Terms_use.cfm

8. Glabbeek, F.V., Riet, R.P.V., Baumfeld, J.A., Neale,P.G., O'Driscoll, S.W., Morrey, B.F., & An, K.N. (2004). Detrimental effect of overstuffing or understuffing with a radial head replacement in the medial collateral-ligament deficient elbow. The Journal of Bone and Joint Surgery, Incorporated, 86-A (12), 2629-2635.

9. Beingessner, D.M., Dunning, C.E., Gordon, K.D., Johnson, J.A., & King, G.J.W. (2004). The effect of radial head excision and arthroplasty on elbow kinematics and stability. The Journal of Bone and Surgery, Incorporated, 86-A (8), 1730-1739.

10. Beingessner, D.M., Dunning, C.E., Gordon, K.D., Johnson, J.A., & King, G.J.W. (2005). The effect of radial head fracture size on elbow kinematics and stability. Journal of Orthopaedic Research, 23 (2005), 210-217.

11. Dunning, C.E., Duck, T.R., King, G.J.W., & Johnson, J.A. Simulated active control produces repeatable motion pathways of the elbow in an in vitro testing system. The Journal of Biomechanics, 34 (2001), 1039-1048.

12. A Patient's Guide to Elbow Anatomy. (2003). Retrieved October 29 2007, from eOrthopod:

http://www.eOrthopod.com

13. Glabbeek, F.V., Riet, R.P.V., Baumfeld, J.A., Neale, P.G., O'Driscoll, S.W., Morrey, B.F., & An, K.N. The kinematic importance of radial neck length in radial head replacement. Medical Engineering & Physics, 27 (2005), 336-342.

14. Bernard F. Morrey, S. T.-N. (1989). Valgus Stability of the Elbow: A definition of Primary and Secondary Constraints. Journal of Clinical Orthopaedics and Related Research , 187-194.

15. Wolff AL, H. R. (2006). Lateral elbow instability: nonoperative, operative. Journal of Hand Therapy , 238-243.

16. Postures and Direction of Movement. (2005). Retrieved October 29, 2007, from Medical Training Resources: http://www.medtrng.com/posturesdirection.htm

17. M. Margareta, V. F. (2001). Biomechanics of the Elbow. In J. Butler, Basic Biomechanics of the Musculoskeletal System (pp. 340-355). Baltimore: Lippincott Williams & Wilkins.

18. Tan, V. (2007, October). Hand, Upper Extremity & Microvascular Surgery. Retrieved October 29, 2007, from American Academy of Orthopaedic Surgeons: http://www.orthdoc.aaos.org/VirakTanMD/

19. Flock of Birds: Position and Orientation Measurement System. (1999, January 18). Burlington, Vermont, United States of America. Retrieved February 11, 2007, from Flock of Birds Ascension Technology Corporation.

20. Joseph Hamill, W. S. (2004). Three Dimensional Kinematics . In G. E. D. Gordon E. Robertson, Research Methods in Biomechanics (pp. 35-52). Amherst: Library of Congress Cataoging-in-Publication Data.

21. Janine E. Pierce, G. L. (2005). Muscle forces predicted using optimization methods are coordinate. Journal of Biomechanics, 695-702.